



Australian Government

Ansto

Nuclear-based science benefiting all Australians



Reactor-based time-of-flight SANS instrument BILBY: accumulated experience in collecting scattering from samples of various nature, dealing with incoherent backgrounds and complex transmissions along with solving issues in non-trivial data reduction

Anna Sokolova

Andrew E. Whitten and Liliana de Campo

Australian Centre for Nuclear Scattering

Australian Nuclear Science and Technology Organisation

Project history

October 2009

General design concept

December 2013

Commissioning licence granted by ARPANSA

1 March 2014

Neutrons on detectors are recorded,
hot commissioning started

January 2016

In operation

fourth cycle in operation (from July, 2017)

Brief project history

BILBY: **started October, 2009**
 A\$11M, 5 years
 design, procurement, installation, commissioning

- Design – Jason Christoforidis
- Engineering – Andrew Eltobaji
- Mechanical – John Barnes and mechanical team
- Electrical – Frank Darmann and EE team
- DAE – Andrew Berry and DAE team
- Data reduction and collection software – Nick Hauser group
- Procurement – Craig Ross

Instrument scientists (started mid 2014):

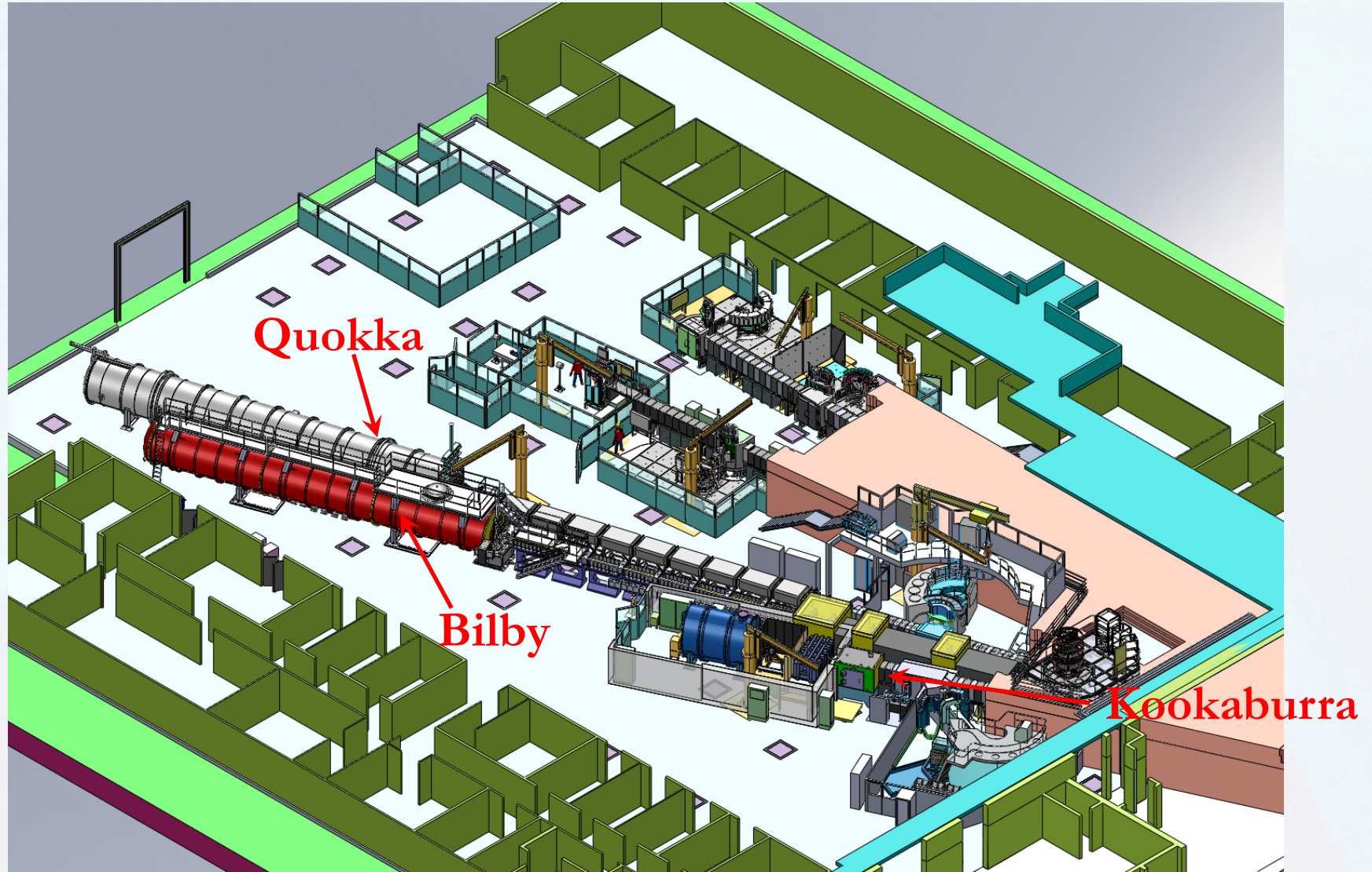
Dr Andrew Whitten, Dr Liliana de Campo

Hot commissioning: End 2015

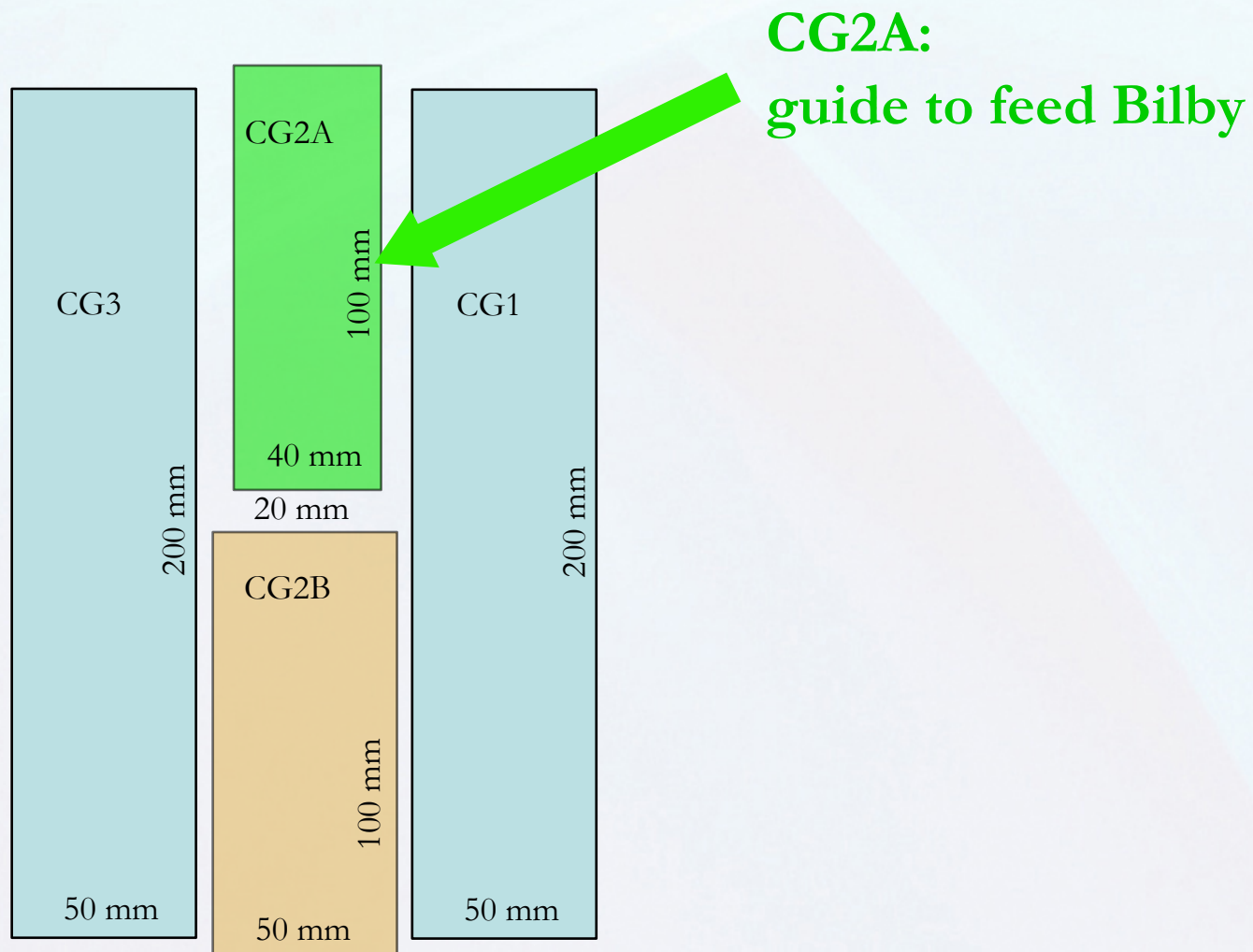
Robert Knott
Elliot Gilbert
Katy Wood
Bill Hamilton
Glenn Ford
David Howes
Phil Bentley

HMI
ILL
Saclay
NIST
SNS
ISIS

ACNS: Neutron Small Angle Scattering

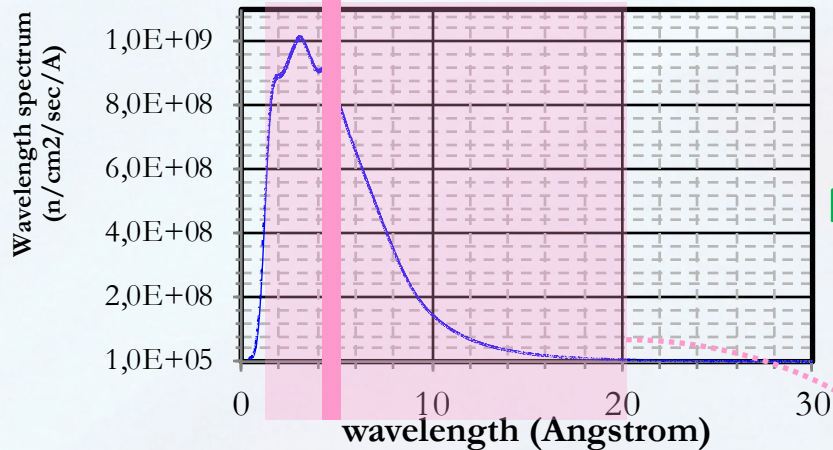


ANSTO: Guides looking at the cold source

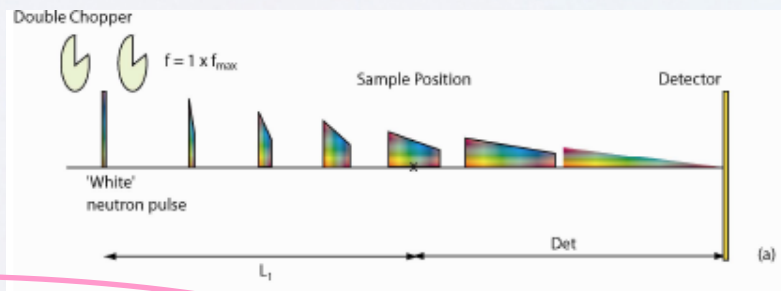


Monochromatic vs polychromatic SANS

Cold spectrum



NO time structure in neutron flow

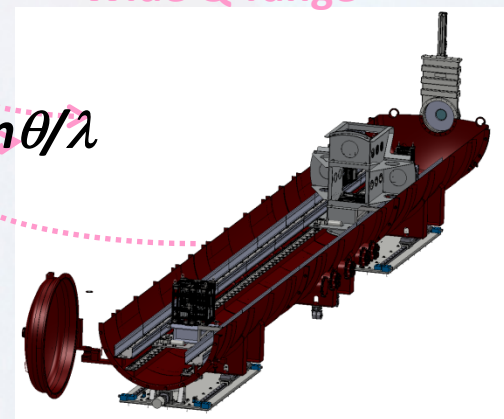


TIME structure in neutron flow

Wide Q-range

$$I(Q)$$

$$Q = 4\pi \sin \theta / \lambda$$



$$\Delta \lambda / \lambda = \Delta D / D$$

Flexible resolution: 10% of mono → 3-30% on poly

Australian Centre for Neutron Scattering: two SANS machines

Quokka:

NVS only

Polarised neutrons

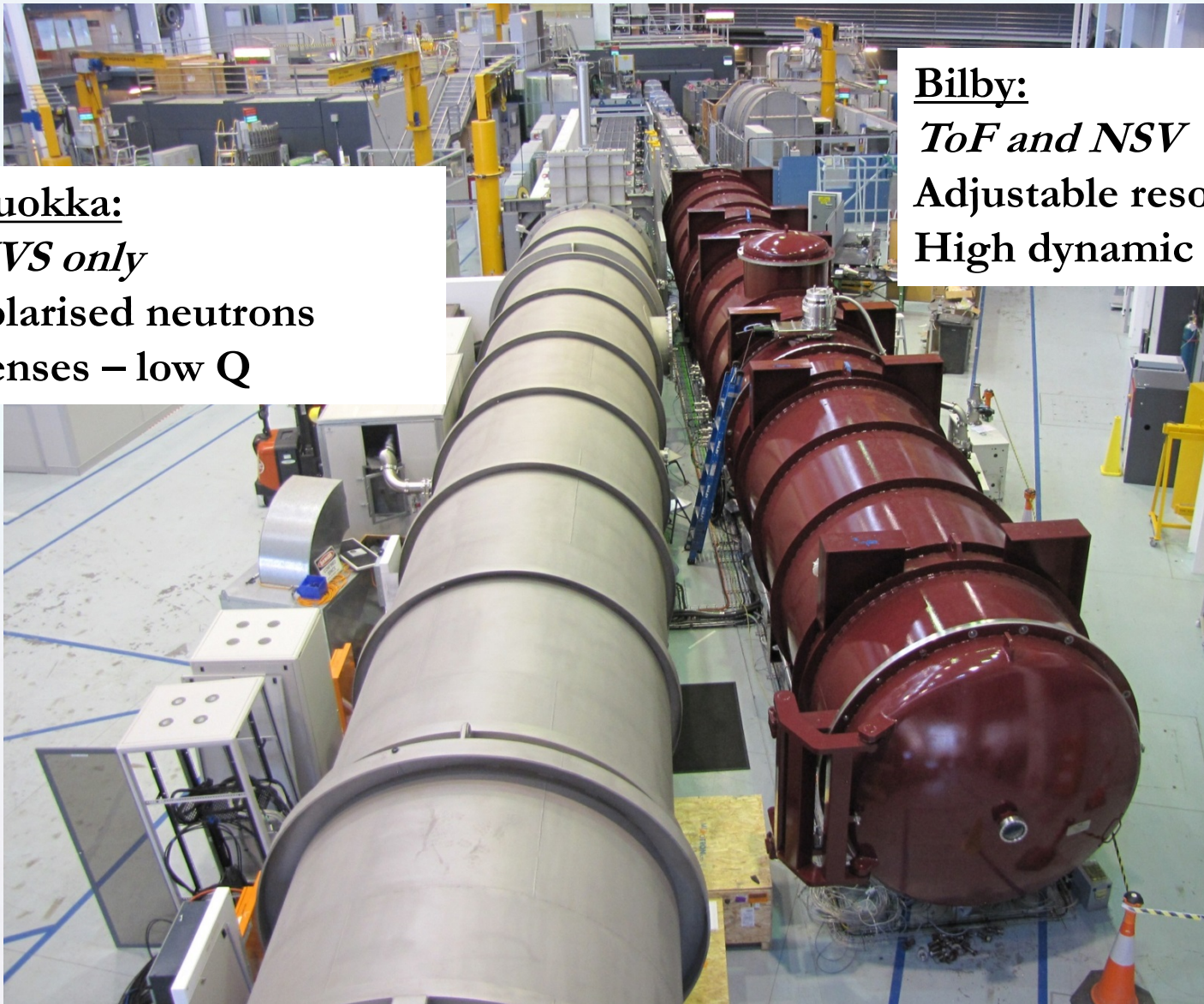
Lenses – low Q

Bilby:

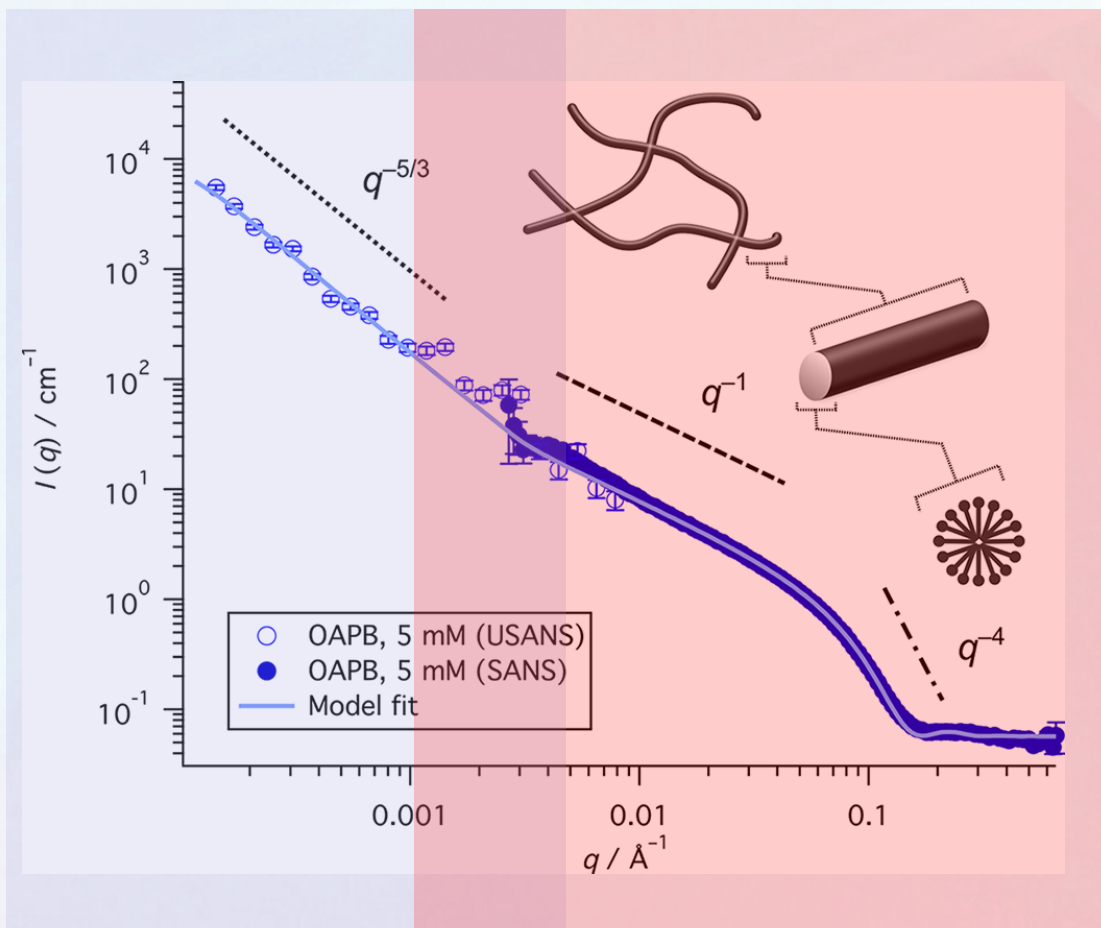
ToF and NSV

Adjustable resolution

High dynamic Q range



Bilby + Kookaburra



SANS data over four decades
in Q (KOOKABURRA & BILBY)

Kelleppan et al, Langmuir 2018

$1 \times 10^{-3} \text{\AA}^{-1}$

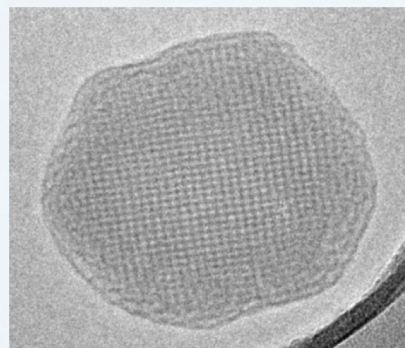
Bilby

1.8\AA^{-1}

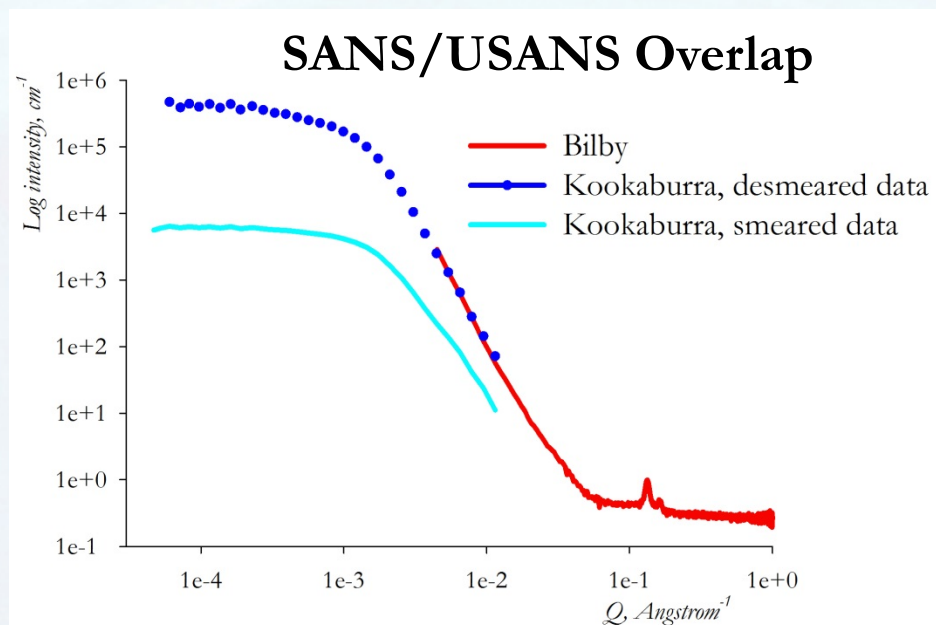
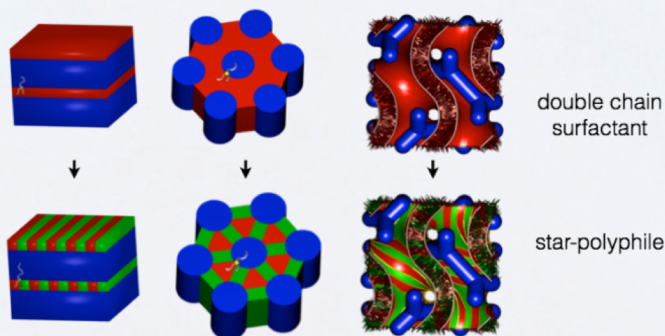
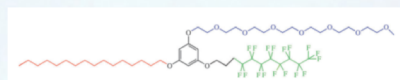
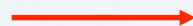
$Q (\text{\AA}^{-1})$

Bilby - large dynamic Q-range in ToF mode

Liquid Crystals based on Star-Polyphiles



Reduction of selected wavelengths (3\AA - 10\AA)



A novel lyotropic liquid crystal formed by triphilic star-polyphiles: hydrophilic/oleophilic/fluorophilic rods arranged in a 12.6.4. tiling

Liliana de Campo et al

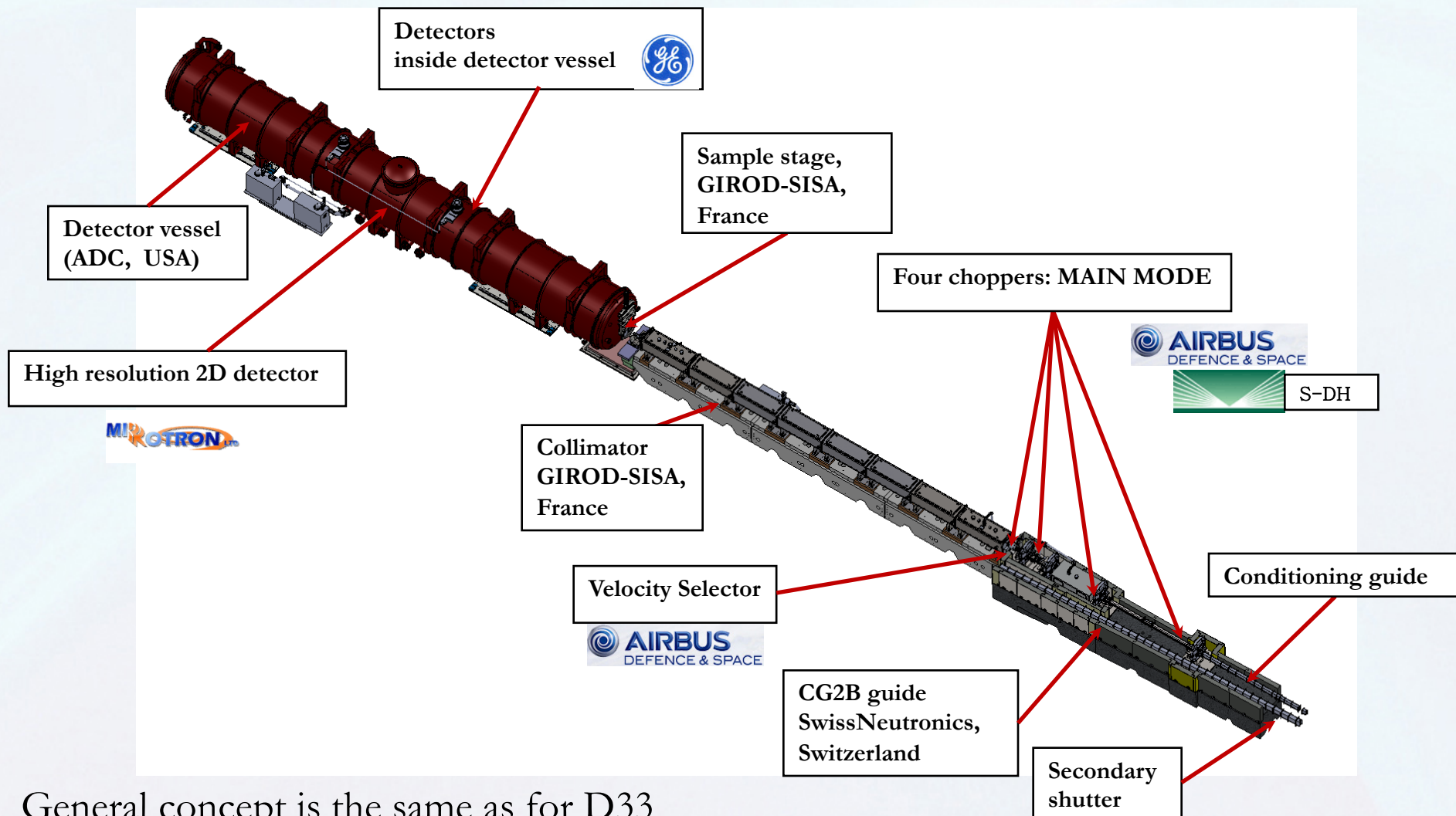
Phys. Chem. Chem. Phys., 2011,13, 3139-3152



Nuclear-based science benefiting all Australians

Representative CryoTEM image taken by L.Waddington (CSIRO), figure courtesy of S.Hyde (ANU) and M. Moghaddam (CSIRO).

Bilby: general layout



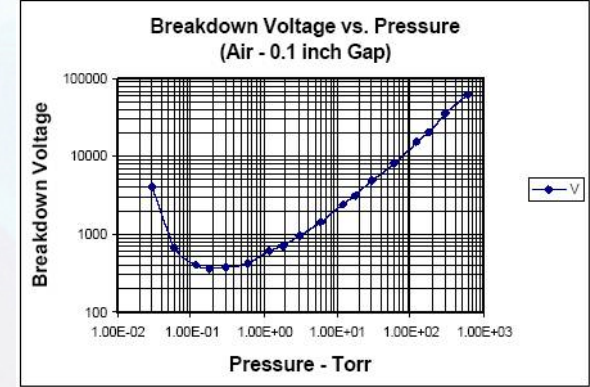
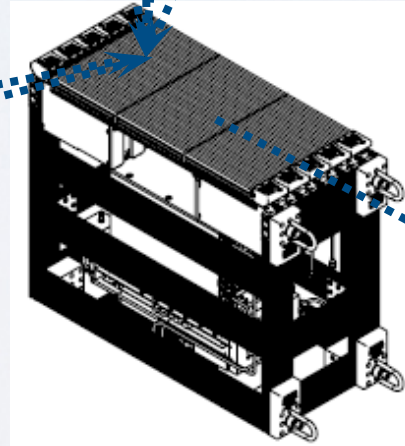
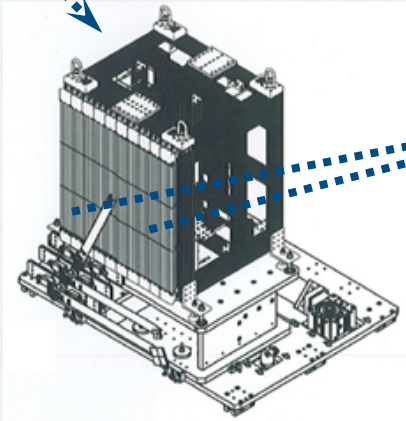
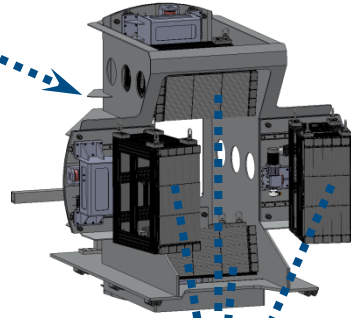
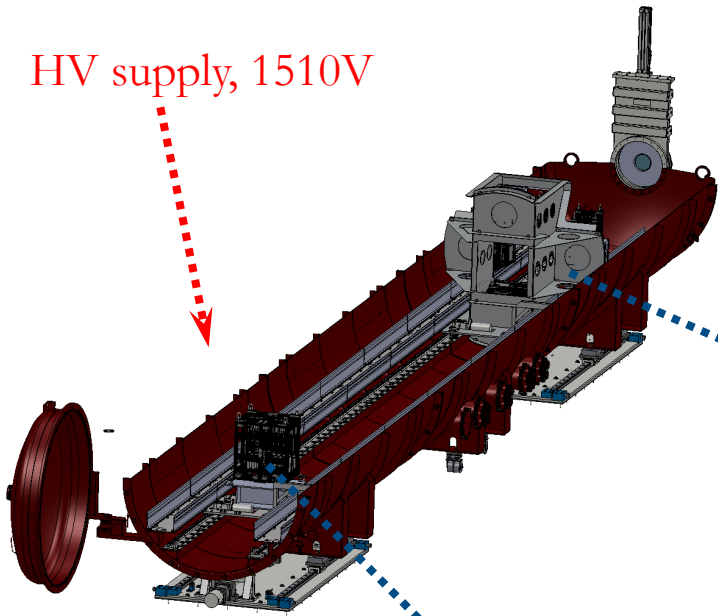
General concept is the same as for D33 machine at ILL

C. D. Dewhurst et al

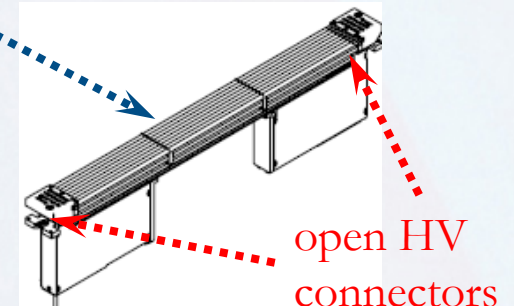
"The small-angle neutron scattering instrument D33 at the Institut Laue-Langevin", J Appl Cryst 2016 49 p.1-14

Detectors

HV supply, 1510V

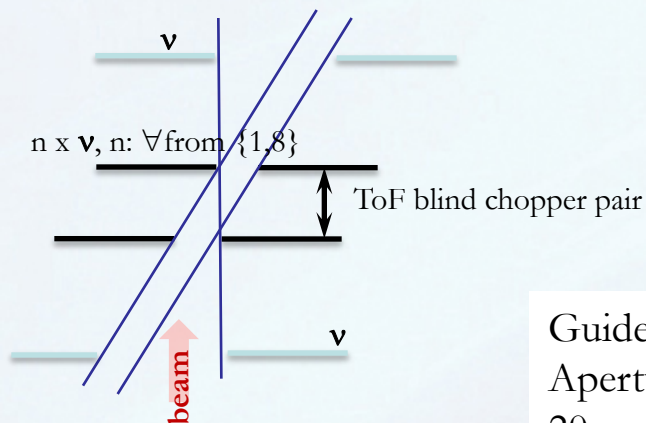


Forbidden region:
 $600 \text{ mbar} \div 1 \cdot 10^{-3} \text{ mbar}$

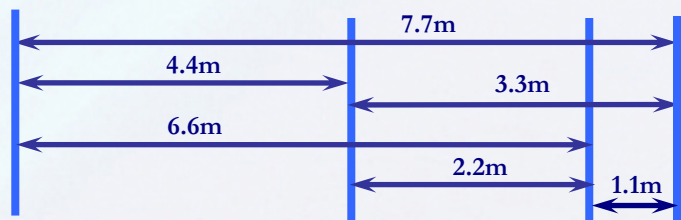


- Entire vessel sits on rails
- Vacuum: $1 \cdot 10^{-4} \text{ mbar}$ (with confidence, $\sim 30 \text{ hours}$)
 - Possibility to open beam at $\sim 700 \text{ mbar}$

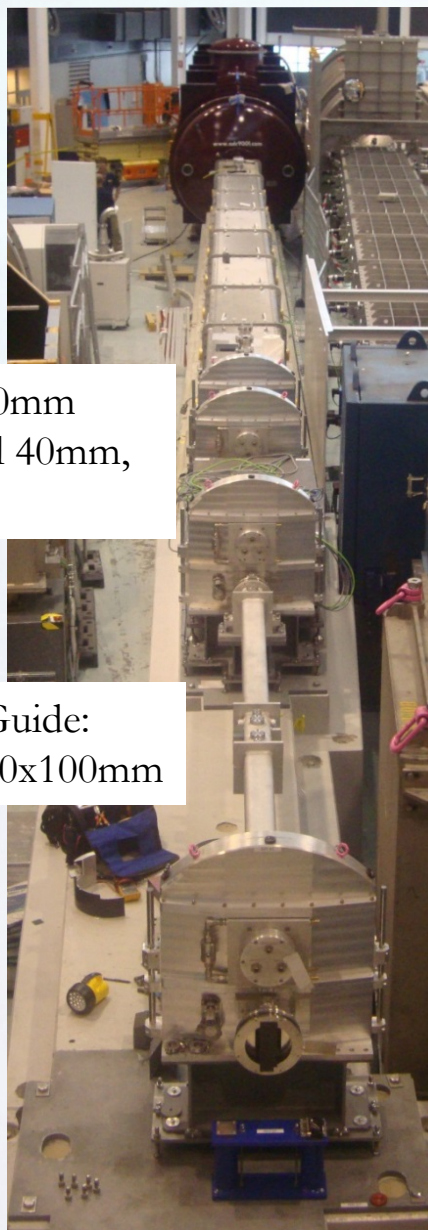
Choppers & Collimator



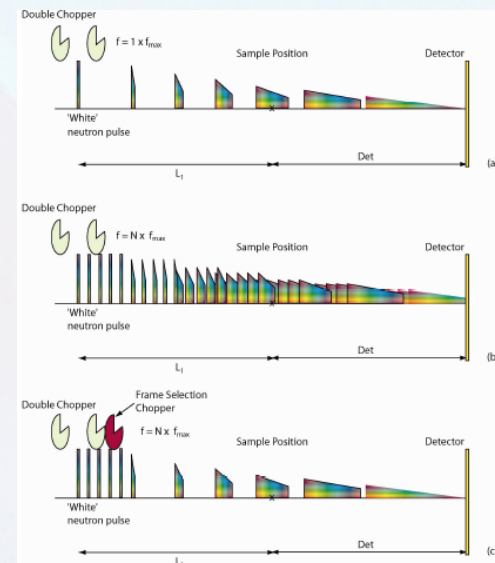
Guides: 40x40mm
Apertures: incl 40mm,
20mm, 10mm



Guide:
40x100mm



$$\frac{\Delta\lambda}{\lambda} = \frac{\Delta t}{t} = \frac{\Delta D}{D}$$



- Low resolution:

- porosity, large biomacromolecules etc

- High resolution:

- liquid crystals, polymers etc

$$\lambda: 2\text{\AA} \div 20\text{\AA}$$

$$\Delta\lambda/\lambda: 4\% \div 30\%$$

Data reduction

Main equation:

$$I(Q) = \frac{1}{d_{sam}} \cdot \frac{\sum_{R, \lambda \in Q} C_{sam, corr}(R, \lambda)}{M \cdot \sum_{R, \lambda \in Q} T_{corr}(\lambda, R) \cdot \left[\frac{I_{empty_beam}(\lambda)}{(M_{empty_beam} \cdot att_{empty_beam})} \right] \cdot \Omega(R) \cdot Det_{flood}(R)}$$

Important: to reduce data on different wavelength ranges

Pixel size: 8mm x 2.7mm

Deadtime, beam monitor, detector efficiency: no correction

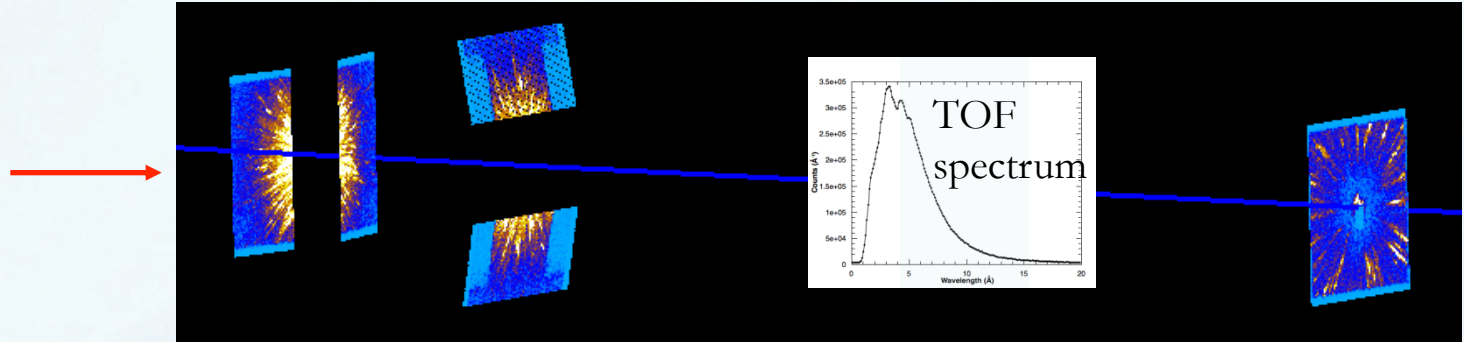
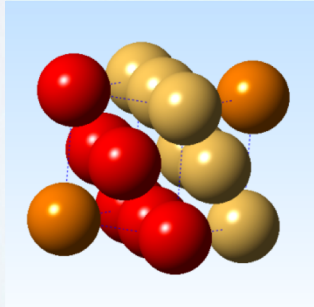
Software: www.mantidproject.org

*O. Arnold, et al., Mantid—Data analysis and visualization package for neutron scattering and μ SR experiments, Nuclear Instruments and Methods in Physics Research Section A, **764**, 2014, p.156-166*

Bilby - in ToF mode at high resolution ($\sim 4.5\% \Delta\lambda/\lambda$)

Sample

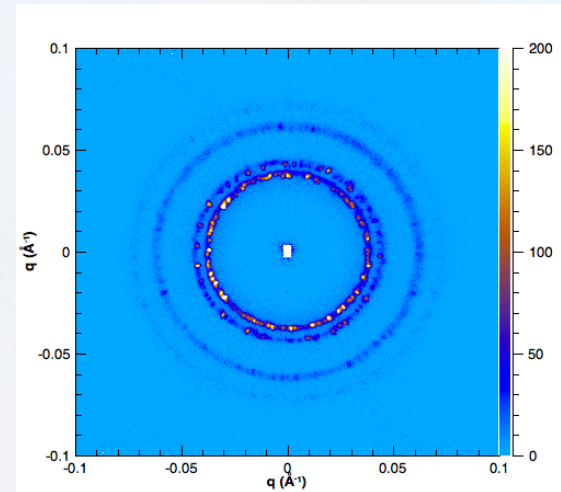
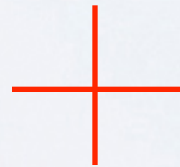
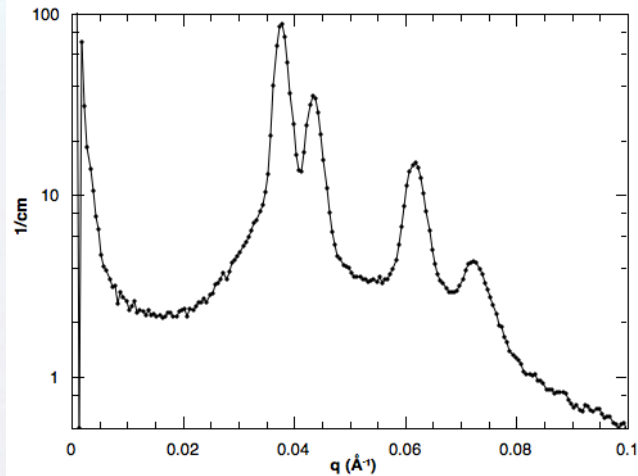
Raw data: (5m SDD to closest curtains, 10m SDD for rear detector)



close packed micelles
block co-polymer F127 + 80% D2O

Reduction of selected
wavelengths (4Å-15Å)

1D data



2D data

Resolution

D.F.R. Mildner & J.M. Carpenter, J. Appl. Cryst. 17(1984)249-256

$$(\sigma_Q)^2 = \frac{1}{12} \left(\frac{2\pi}{\lambda} \right)^2 \left[3 \frac{R_1^2}{L_1^2} + 3 \frac{R_2^2}{L'^2} + \frac{(\Delta R)^2}{L_2^2} + \frac{R^2}{L_2^2} \left(\frac{\Delta\lambda}{\lambda} \right)^2 \right]$$

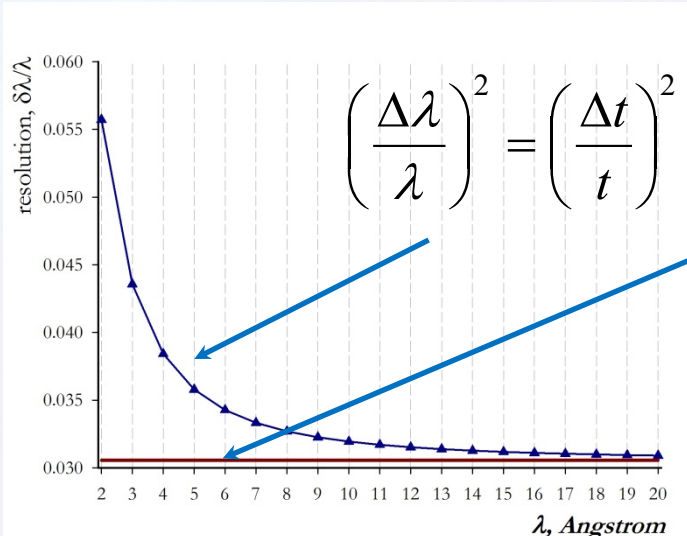
$$\frac{1}{L'} = \frac{1}{L_1} + \frac{1}{L_2}$$

$$\left(\frac{\sigma_Q}{Q} \right)^2 = \frac{4\pi^2}{\lambda^2 Q^2} \left[\left(\frac{R_1}{2L_1} \right)^2 + \left(\frac{R_2(L_1 + L_2)}{2L_1 L_2} \right)^2 + \frac{1}{12} \left(\frac{\Delta R}{L_2} \right)^2 \right] + \frac{1}{12} \left(\frac{\Delta\lambda}{\lambda} \right)^2$$

$$Q \approx \frac{2\pi\theta}{\lambda} \approx 2\pi \frac{R}{\lambda L_2}$$

R. Heenan. ISIS

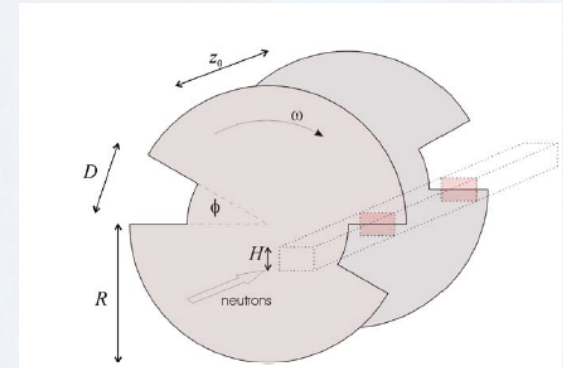
Based on A.A. van Well, H Fredzizke “On the resolution and intensity of a time-of-flight neutron reflectometer”, Physica B, 2005



$$\left(\frac{\Delta\lambda}{\lambda} \right)^2 = \left(\frac{\Delta t}{t} \right)^2 \cong \left\{ \left(\frac{\tau_c}{t} \right)^2 + \left(\frac{\tau_h}{t} \right)^2 \right\}$$

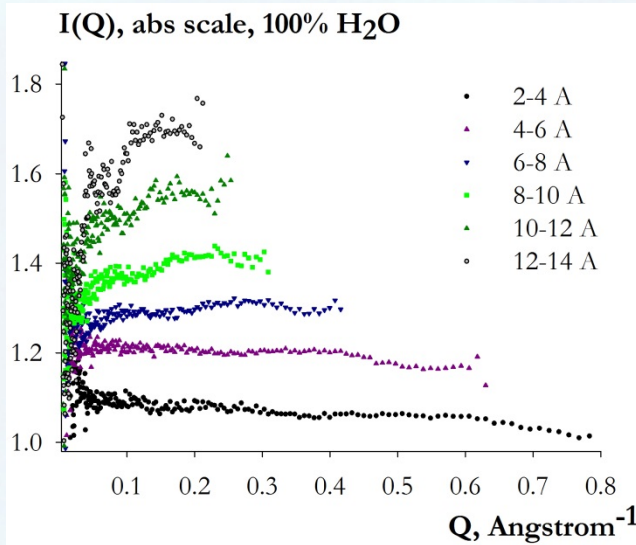
$$\tau_h = D/\omega R \quad \tau_c/t = z_0/L$$

not considering electronics response time and detector' depth



A. Nelson and C. Dewhurst “Towards a details resolution smearing kernel for time-of-flight neutron reflectometers.”, J Appl Cryst 2015

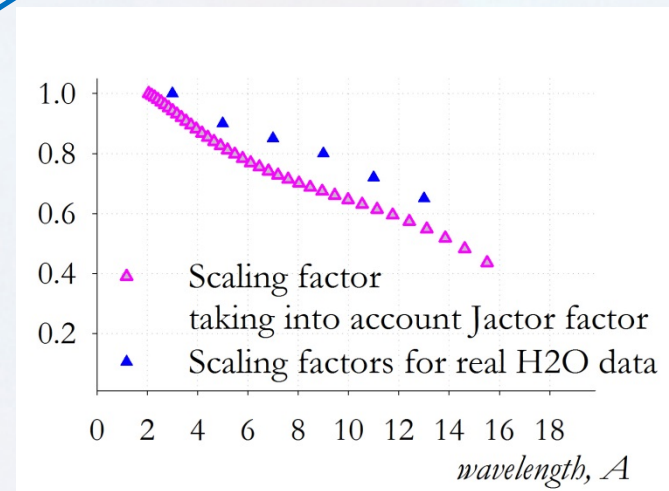
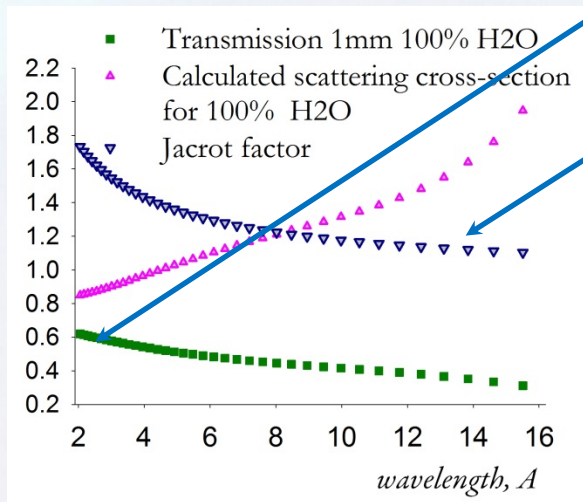
Background: elastic incoherent



$$\frac{d\Sigma}{d\Omega_{inc}} = \frac{g_\lambda}{4\pi} \left[\varphi_H \frac{d\Sigma}{d\Omega_{inc,H_2O}} + (1 - \varphi_H) \frac{d\Sigma}{d\Omega_{inc,D_2O}} \right]$$

$$\left(\frac{d\Sigma}{d\Omega} \right)_{inc} = \frac{1}{4\pi} \frac{1 - T}{tT}$$

$$g_\lambda \cong \frac{1}{\left[1 - \exp\left(-0.6\lambda^{1/2}\right) \right]}$$



“Evaluation of incoherent scattering intensity by transmission and sample thickness”, M. Shibayama et al, J Appl Cryst, 2009

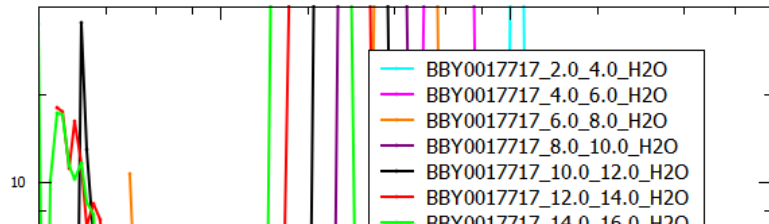
Still a question: to check how seriously we see inelastic component.

Papers on similar issue

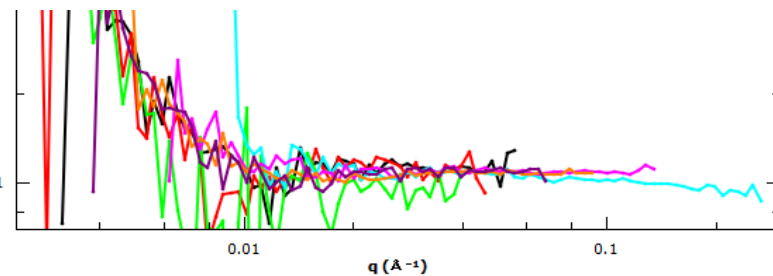
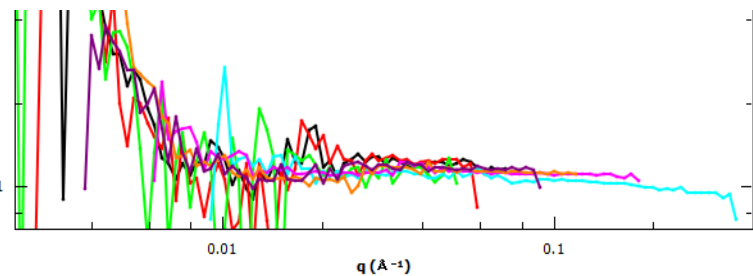
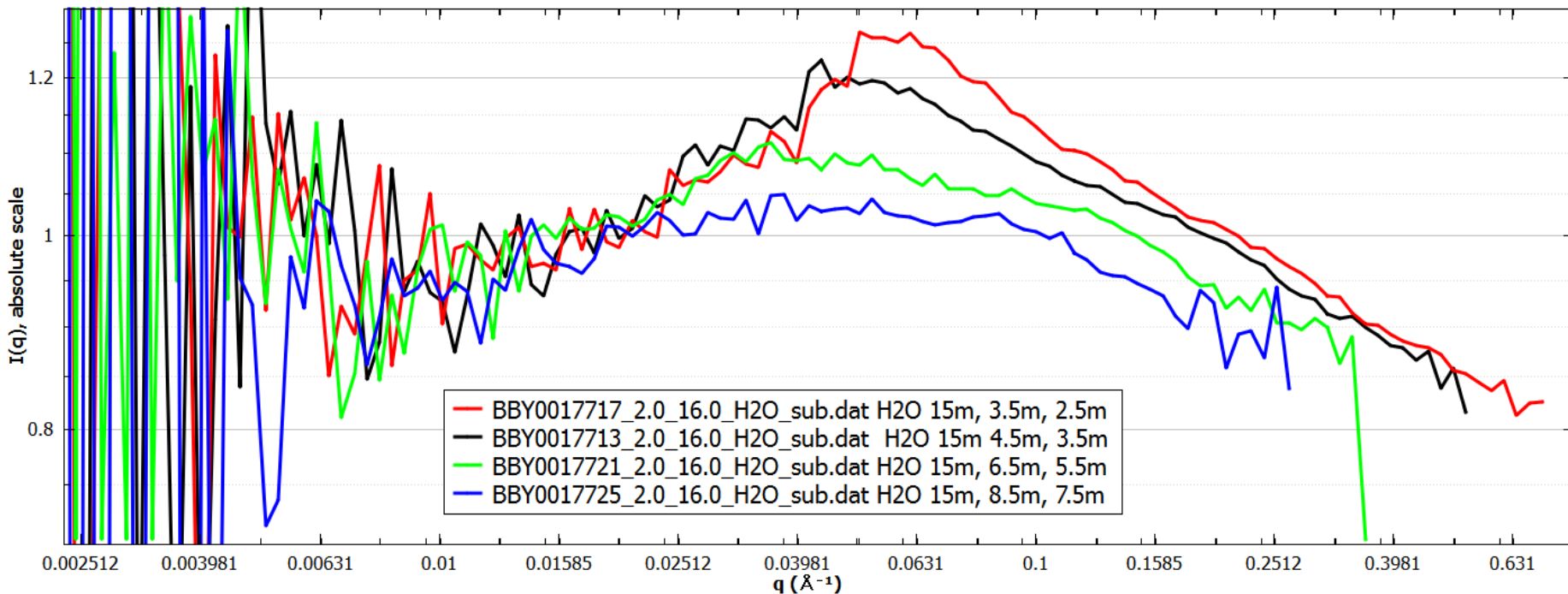
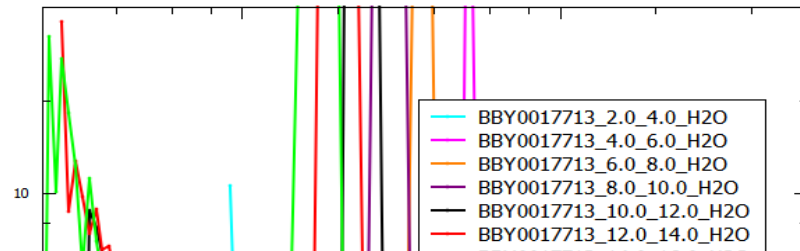
- B Jacrot, G. Zaccai, Biopolymers (1981) 20, 2413-2426
- P. Lindner J Appl Cryst (2000) 33, 807-811
- B. Jacrot 1976
- May, Ibel, Haas 1982 (1-T) correction for H/D mixture
- M. Shibayama 2005; 2009
- J. Barker
- J. Copley 1988
- R.E. Ghosh, A. Rennie, 1990
- A.R. Rennie, R.K. Heenan 1992
- W.S. Dubner, J.M. Schultz 1990
- C. Do, 2014

H2O ToF @ambient

H2O 15m, 3.5m, 2.5m

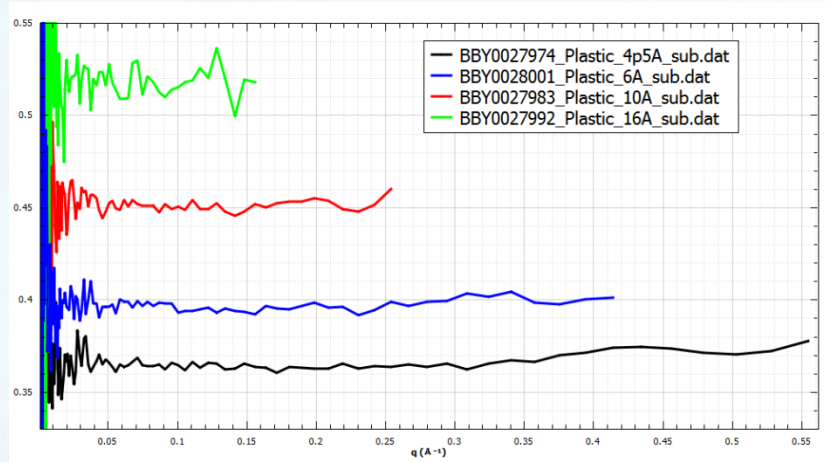


H2O 15m 4.5m, 3.5m

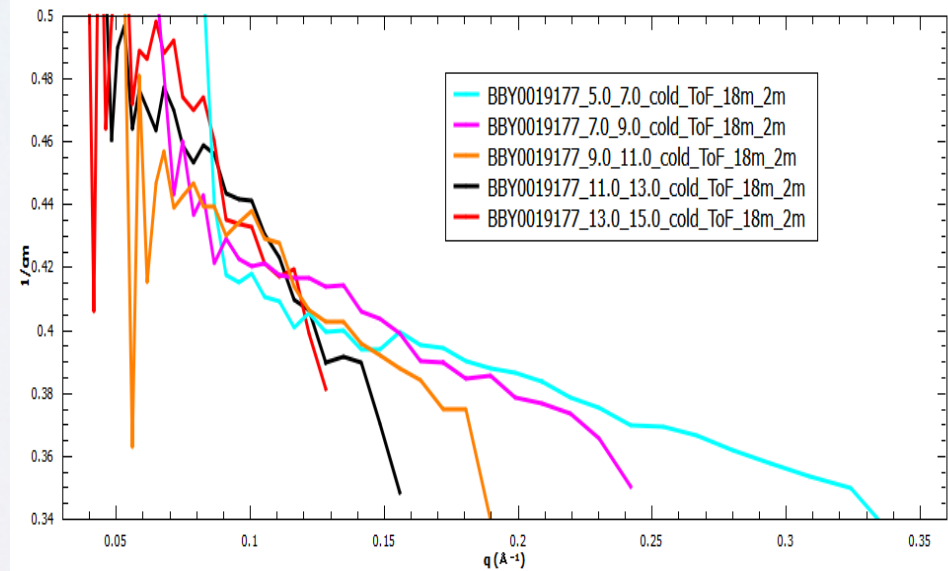
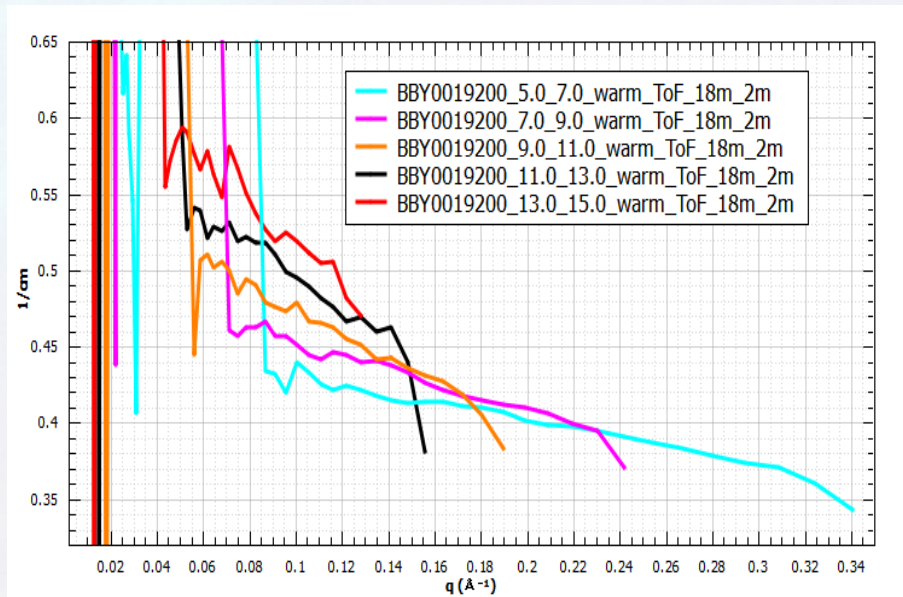


Polycarbonate

NSV Ambient

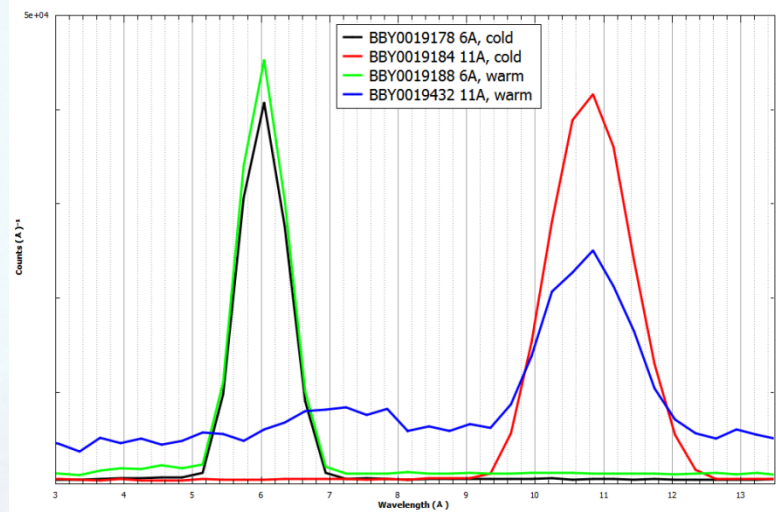


ToF Cold & ambient: cannot see much difference

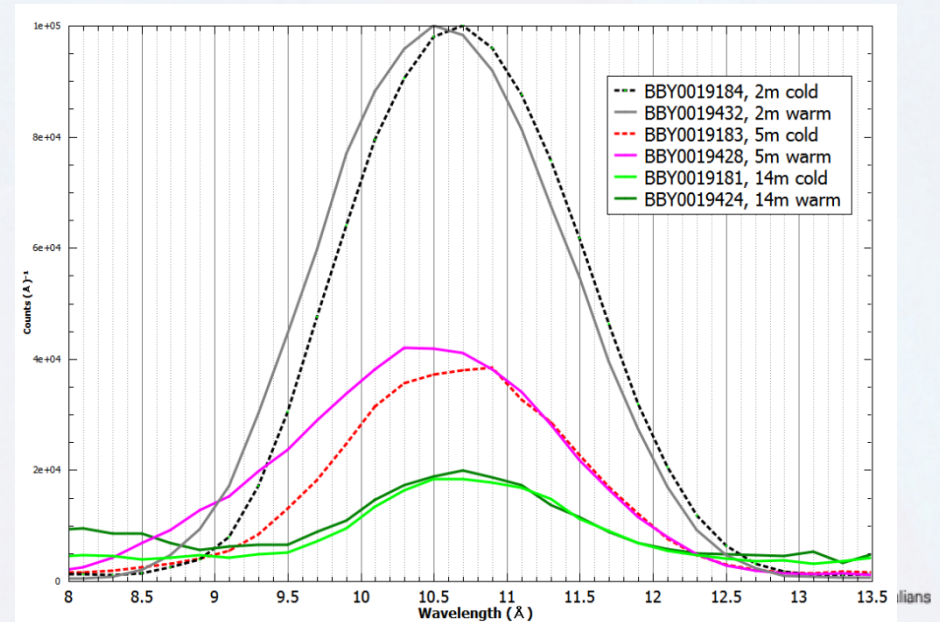
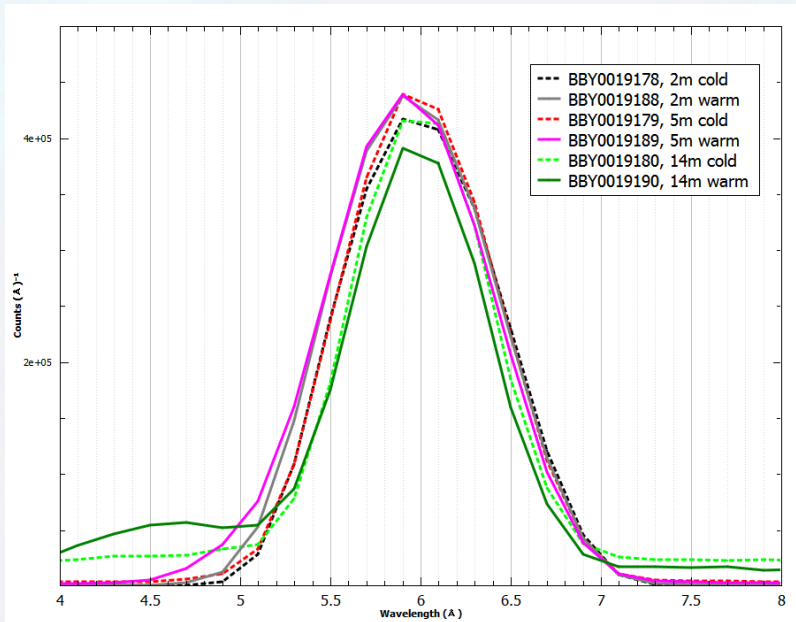


Polycarbonate

ToF wavelength spectrum. rear detector only



ToF wavelength spectrum, curtains only



Background: selected wavelengths – in advance

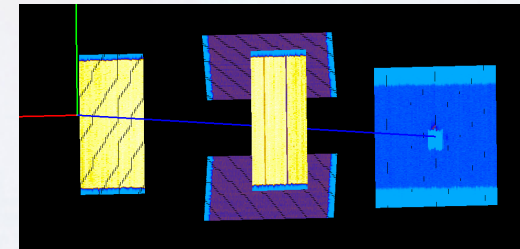
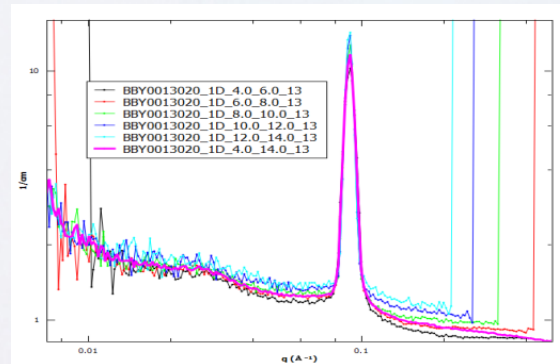
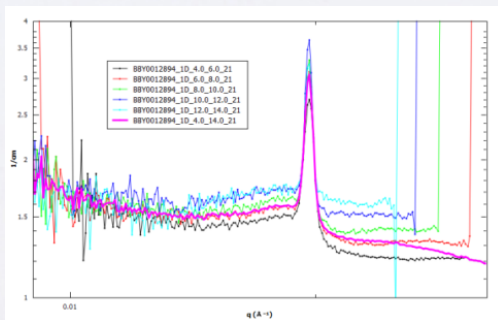
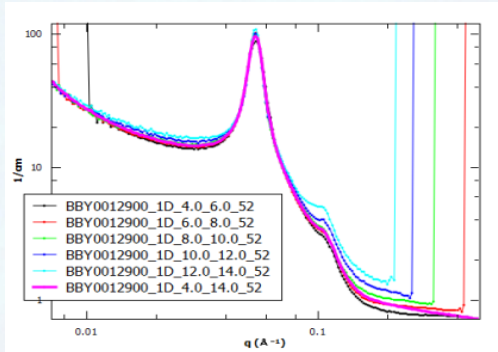
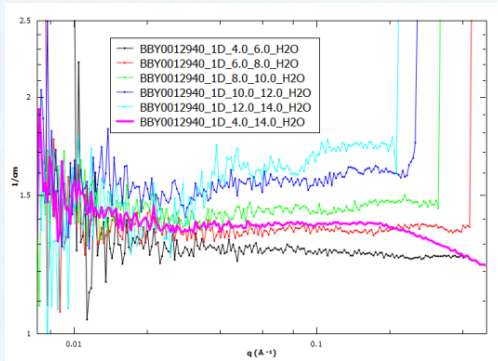
Dr Rico Tabor, Monash University, Melbourne, Australia

Hydrogen from the sample:
how serious the influence is?

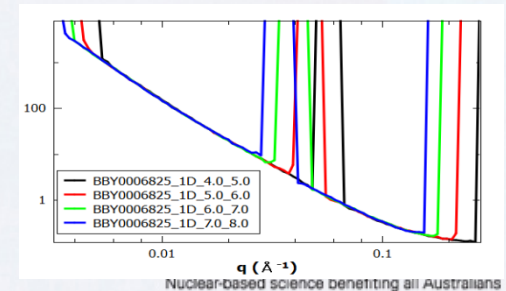
How to subtract ?

ToF – only middle wavelengths
to cover desirable Q

Careful: wavelengths stitching in the background

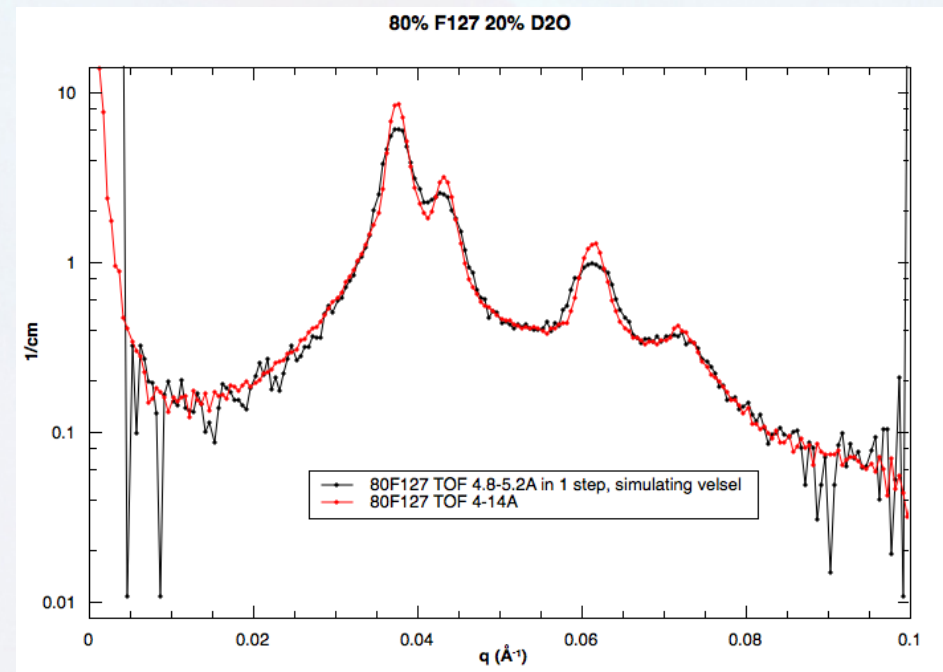
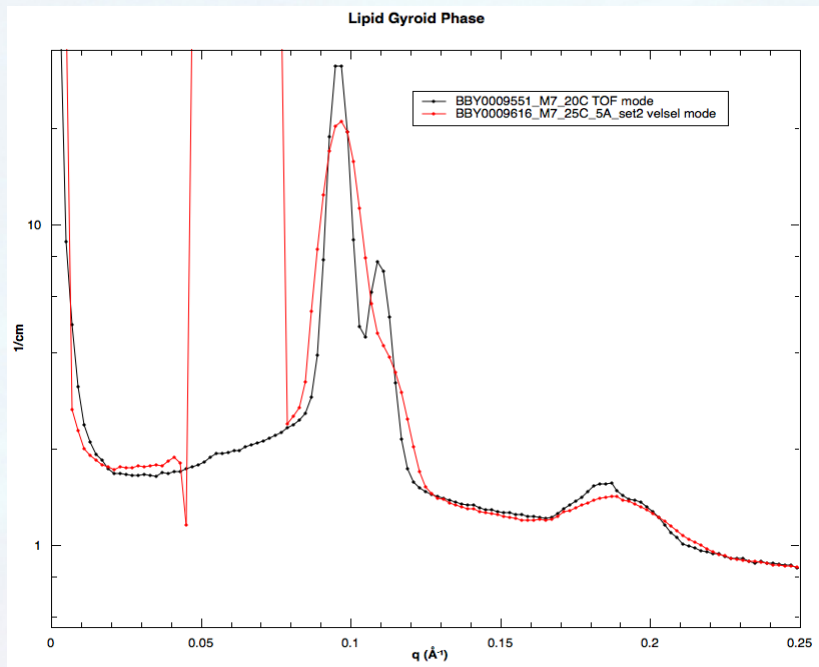


$$q = 4\pi \sin\theta / \lambda$$



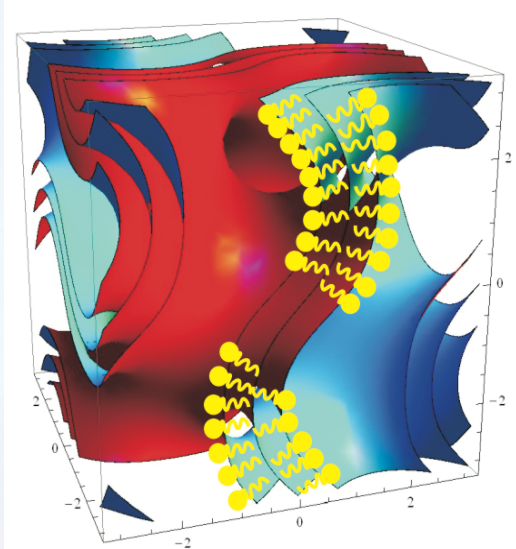
Non-conventional set-up: NVS + ToF simultaneously

Making peaks bright and sharp
eliminating background issue, sacrificing flux



Single transmembrane peptides during in meso crystallization

Charlotte Conn, Leonie van't Hag, Liliana de Campo, Raffaele Mezzenga



- Viscoelastic properties similar to biological membranes
- Flexible structure can partially adapt to accommodate the protein
- Able to incorporate high protein loading
- Protein can diffuse across the plane of the bilayer

Conn, C. E.; Drummond, C. J. *Soft Matter* **2013**, 9 (13) 3449-3464

Conn, C.E. et al. *Soft Matter* **2010**, 6, (19), 4838-4846

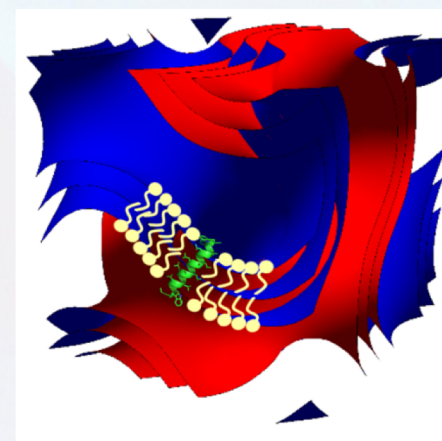
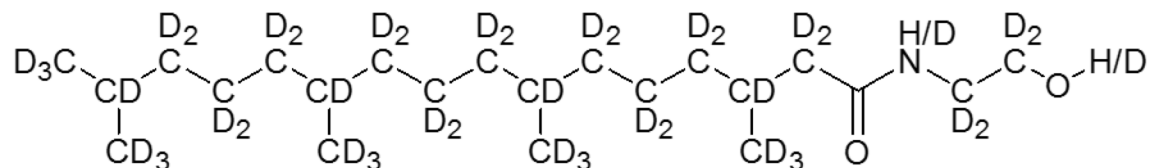
Conn, C.E. et al. *Soft Matter* **2010**, 6, (19), 4828-4837

What is the mechanism of crystal growth?

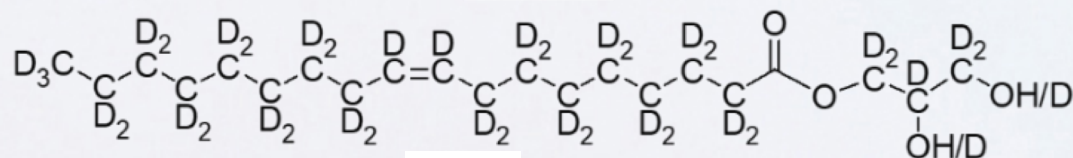
How is this impacted by the nanostructure of the cubic phase?

Single transmembrane peptides during in meso crystallization

Matrix: D-PE (phytanoyl monoethanolamide)



Matrix: D-MO (monoolein)



van 't Hag et al. *J. Phys. Chem. Lett.* 2016 7 (14) 2862-2866

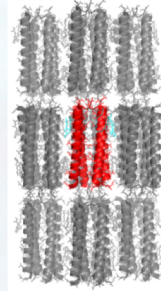
van 't Hag et al., *Langmuir*, 2019

Ansto

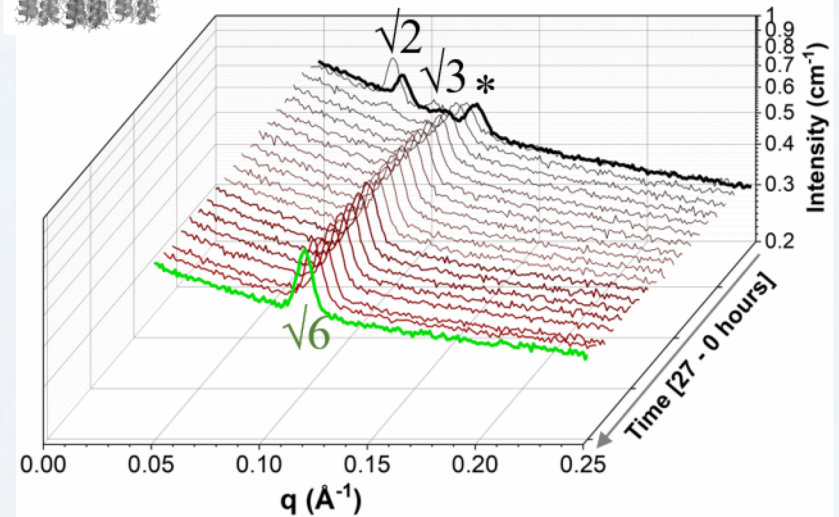
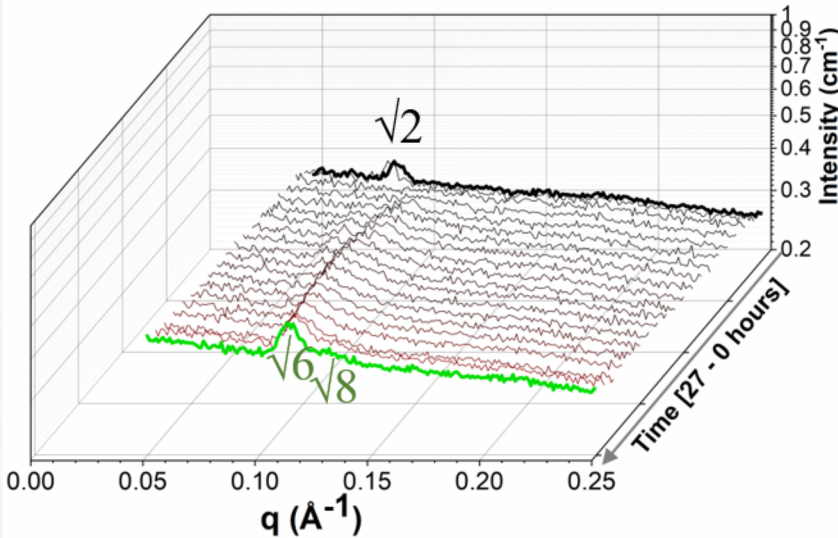
Nuclear-based science benefiting all Australians

Single transmembrane peptides during in meso crystallization

No peptide, MO9 cubic matrix



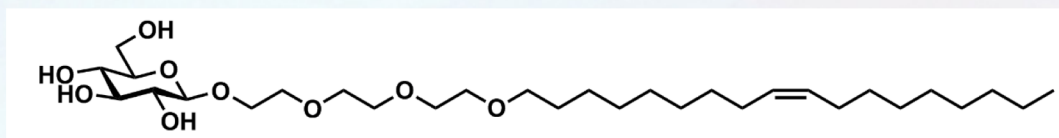
DAP12, peptide



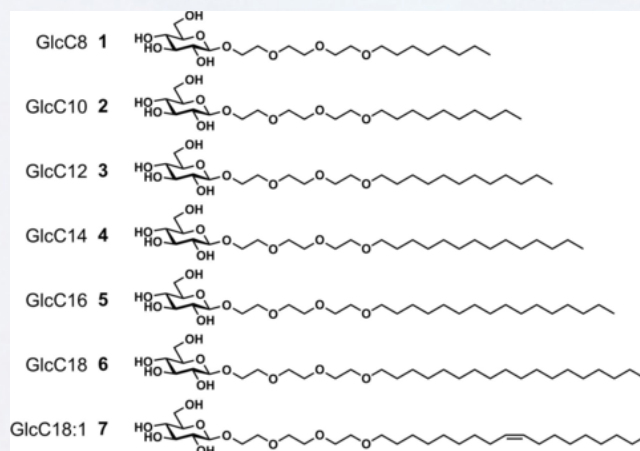
- Transition from diamond cubic phase to gyroid cubic phase (effect of screen)
- More contrast so higher peak intensity. Scattering is mainly from the peptide.
- Variations in peak intensity reflect peptide behaviour.

Wormlike micelle formation of novel alkyl-tri (ethylene glycol)-glucoside carbohydrate surfactants: structure–function relationships and rheology

Aim: To synthesise and characterise new carbohydrate-based surfactants with a focus on potential applications.

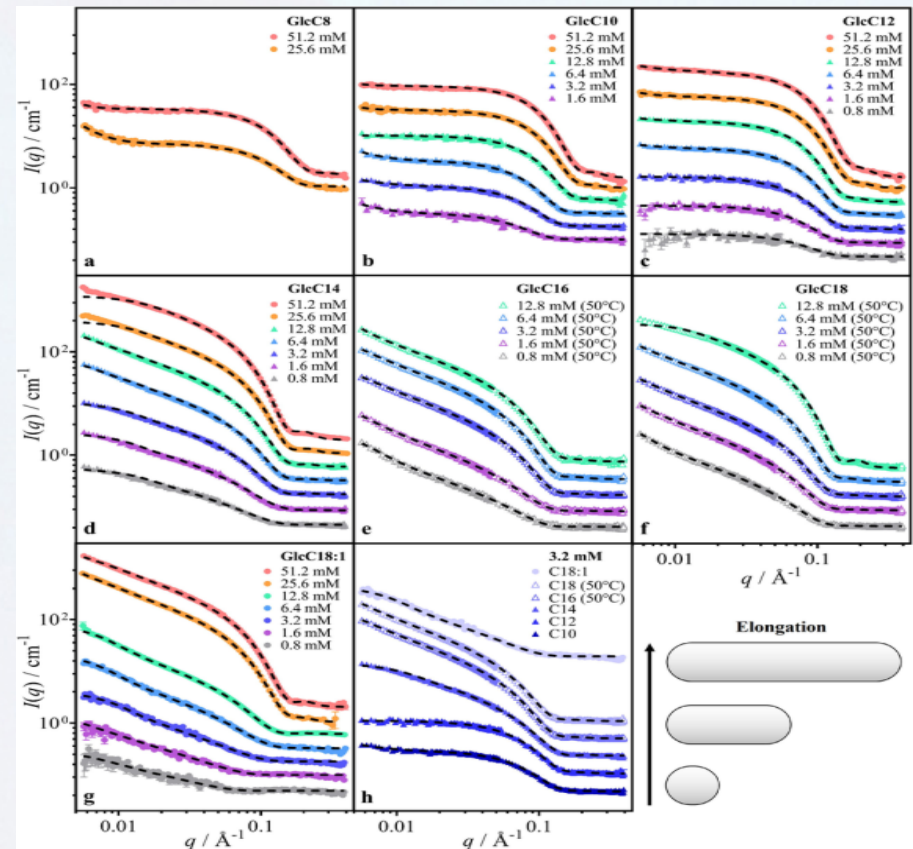


Sugar ——— tri(ethylene glycol) ——— alkyl



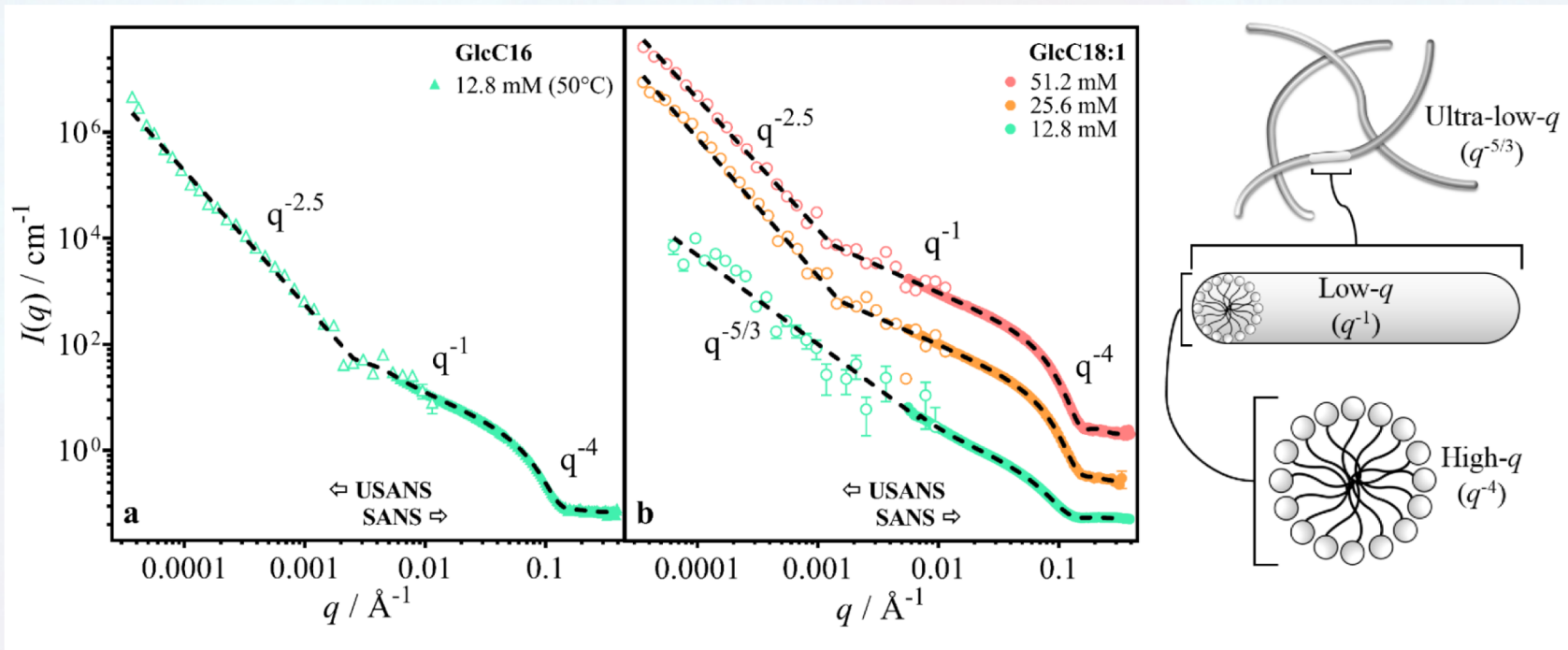
Wormlike micelle formation of novel alkyl-tri (ethylene glycol)-glucoside carbohydrate surfactants: structure–function relationships and rheology

- Short chain (C8, C10) form spherical micelles
- C12 starts to elongate
- C14 pronounced rods
- C16/C18 Krafft point $\sim 45^\circ\text{C}$; insoluble at 25°C , long cylinders/worms @ 50°C
- C18:1 worms @ 25°C !
In summary: increasing tail length increases effective packing parameter = spheres \rightarrow rods \rightarrow worms
- *cis* unsaturation decreases crystallinity

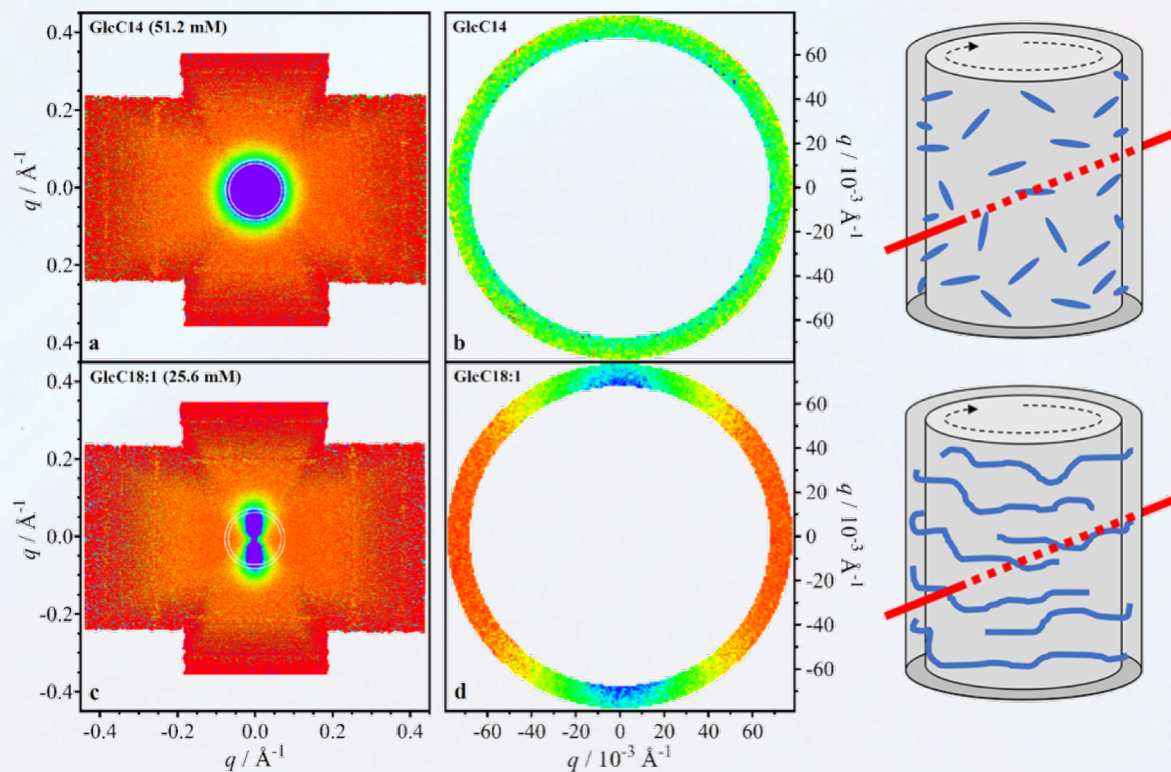


Wormlike micelle formation of novel alkyl-tri (ethylene glycol)-glucoside carbohydrate surfactants: structure–function relationships and rheology

- **USANS allows exploration of wormlike micelles at longer length-scales**



Wormlike micelle formation of novel alkyl-tri (ethylene glycol)-glucoside carbohydrate surfactants: structure–function relationships and rheology



C14 tail = rods
No alignment
under shear

C18:1 tail = worms
Strong alignment under
shear

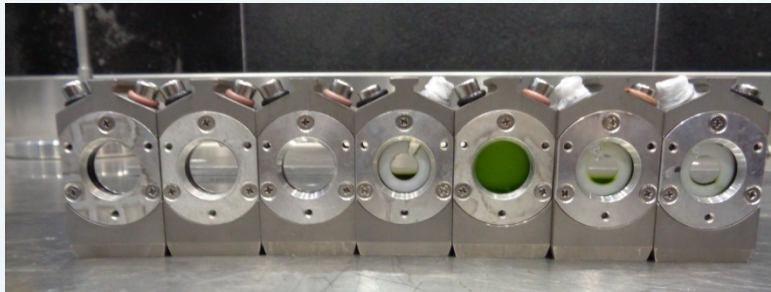
Photosynthetic systems in cyanobacteria & leaves

Jacob J K Kirkensgaard (University of Copenhagen, Denmark)

Kell Mortensen (University of Copenhagen, Denmark)

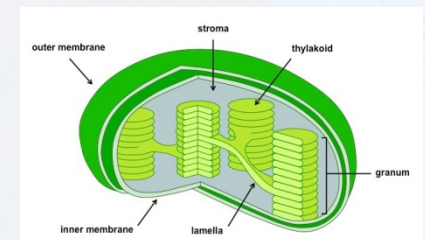
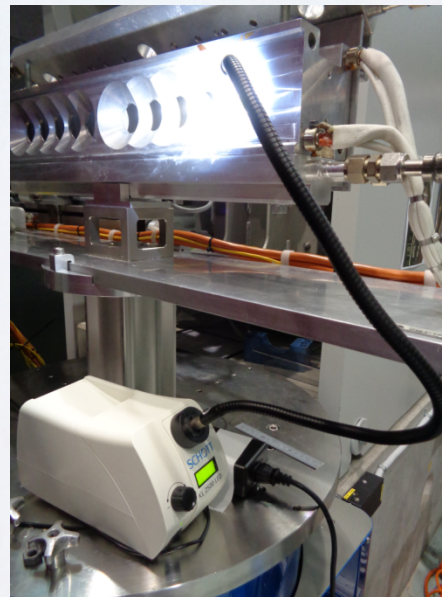
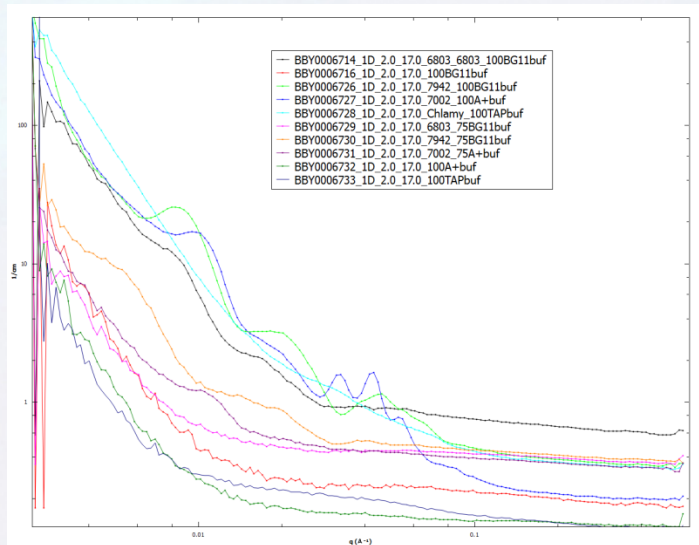
Dainius Jakubauskas (University of Copenhagen, Denmark)

Chris Garvey (ANSTO, Quokka instrument)



Preliminary work:
Optical microscopy

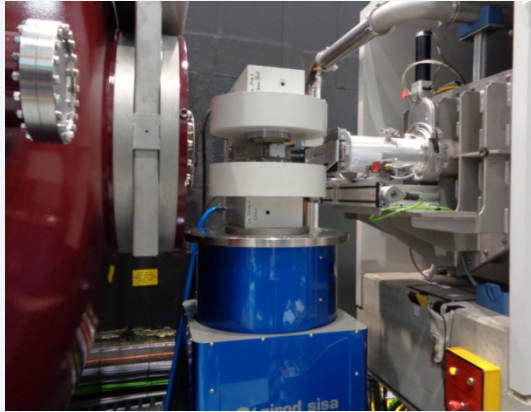
SANS: characteristic distances inside thylakoids



Carbide precipitation kinetics in cryogenically treated tool steels

Nicole Stanford (Monash Uni) & Kathleen Wood (ANSTO)

Ajesh Antony (Deakin Uni) & Thomas Dorin (Deakin Uni)



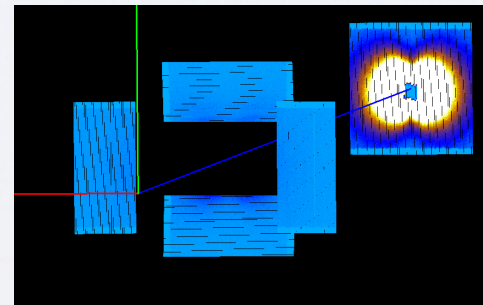
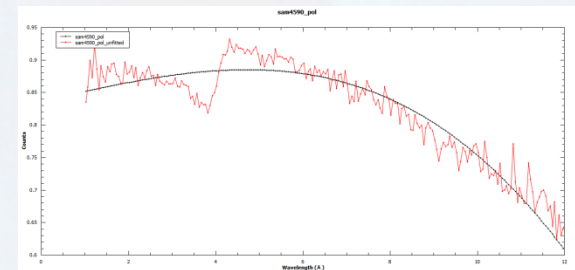
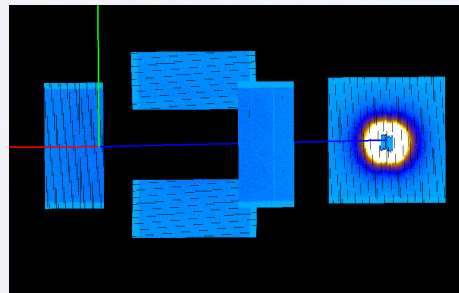
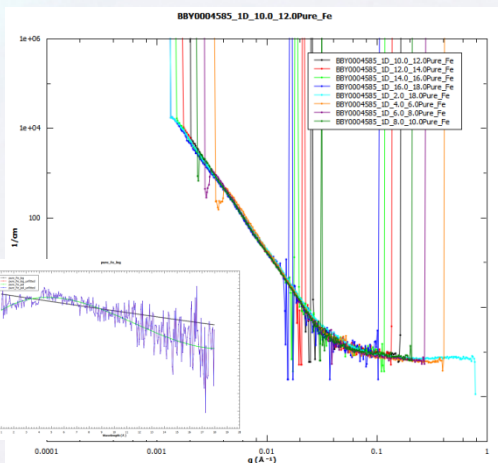
Preliminary work:

Optical microscopy; Lab-scale x-ray diffraction

Transmission electron microscopy;

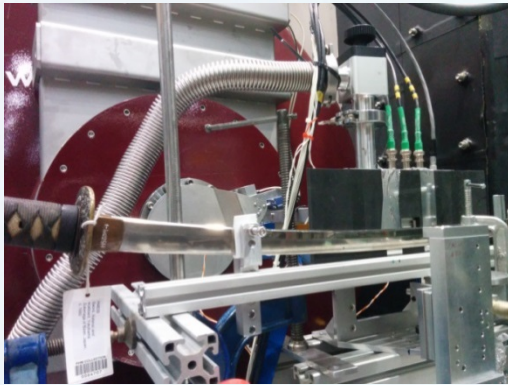
Atom probe tomography

SANS: the size and volume fraction of precipitates @ 1T



Non-standard set-up: imaging with cold neutrons

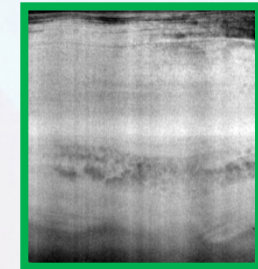
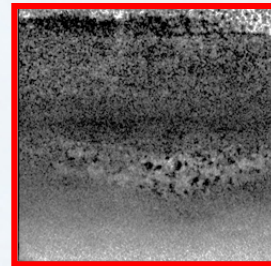
The Samurai Sword



A. Tremsin et al “Energy-resolved neutron imaging options at a small angle neutron scattering instrument at the Australian Center for Neutron Scattering”

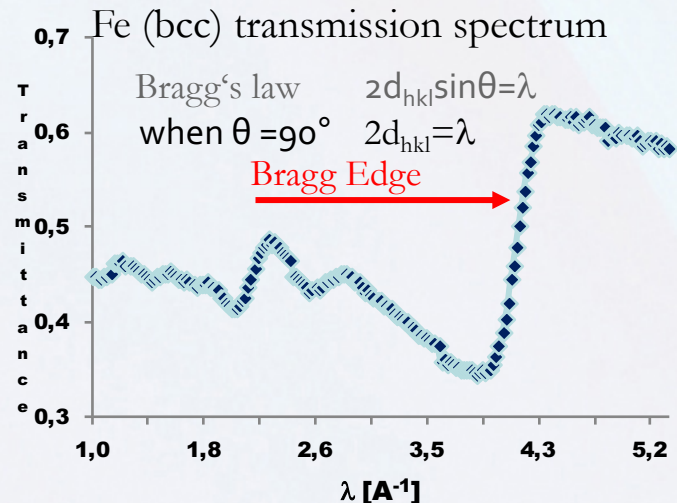
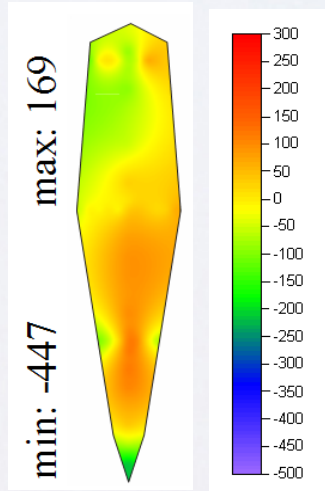
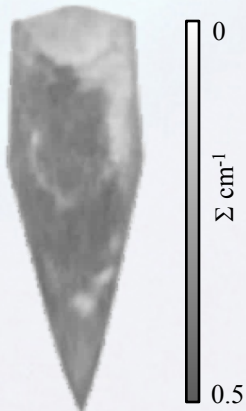
“Review of scientific instruments”, 2019

ToF Bragg-edge transmission analysis



Dingo: Tomographic cross section

Kowari: Residual stress map



- Morphology
- Structure
- Porosities
- Defects
- Stress components
- d_0 -value
- peak width

Shape, magnitude and location of the Bragg edges can be correlated to texture, crystalline phase, crystallite size, and lattice strain

Bilby papers (those with pages)

1. Dorishetty, P; Balu, R; Sreekumar, A; De Campo, L; Mata, JP; Choudhury, NR and Dutta, NK, Robust and Tunable Hybrid Hydrogels from Photo-Cross-Linked Soy Protein Isolate and Regenerated Silk Fibroin, *ACS Sustainable Chemistry and Engineering* **7**(10), 9257-9271 (2019) (from BILBY, KOOKABURRA, QUOKKA) [DOI](#)
2. Kihara, S; van der Heijden, NJ; Seal, CK; Mata, J; Whitten, AE; Köper, I and McGillivray, DJ, Soft and hard interactions between polystyrene nanoplastics and human serum albumin protein corona, *Bioconjugate Chemistry* **30**(4), 1067-1076 (2019) (from BILBY) [DOI](#)
3. Loy, CW; Matori, KA; Zainuddin, N; Whitten, AE; de Campo, L; Nasir, NIM; Pallan, NFB; Zaid, MHM; Zarifah, NA and Schmid, S, Small Angle Neutron Scattering Study of a Gehlenite-Based Ceramic Fabricated from Industrial Waste, *Solid. State Phenom.* **290**, 22-28 (2019) (from BILBY) [DOI](#)
4. McCoy, TM; King, JP; Moore, JE; Kelleppan, VT; Sokolova, AV; de Campo, L; Manohar, M; Darwish, TA and Tabor, RF, The effects of small molecule organic additives on the self-assembly and rheology of betaine wormlike micellar fluids, *J. Colloid Interface Sci.* **534**, 518-532 (2019) (from BILBY) [DOI](#)
5. Moore, JE; McCoy, TM; Sokolova, AV; de Campo, L; Pearson, GR; Wilkinson, BL and Tabor, RF, Worm-like micelles and vesicles formed by alkyl-oligo(ethylene glycol)-glycoside carbohydrate surfactants: The effect of precisely tuned amphiphilicity on aggregate packing, *J. Colloid Interface Sci.* **547**, 275-290 (2019) (from BILBY, KOOKABURRA) [DOI](#)
6. Sokolova, A; Whitten, AE; de Campo, L; Christoforidis, J; Eltobaji, A; Barnes, J; Darmann, F and Berry, A, Performance and characteristics of the BILBY time-of-flight small-angle neutron scattering instrument, *J. Appl. Crystallogr.* **52**, 1-12 (2019) (from BILBY) [DOI](#)
7. Tremsin, AS; Sokolova, AV; Salvemini, F; Luzin, V; Paradowska, A; Muransky, O; Kirkwood, HJ; Abbey, B; Wensrich, CM and Kisi, EH, Energy-resolved neutron imaging options at a small angle neutron scattering instrument at the Australian Center for Neutron Scattering, *Rev. Sci. Instrum.* **90**(3), 035114 (2019) (from BILBY) [DOI](#)
8. Baek, P; Mata, J. P.; Sokolova, A.; Nelson, A.; Aydemir, N.; Shahlori, R.; McGillivray, D. J.; Barker, D. & Travas-Sejdic, J., Chain Shape and Thin Film Behaviour of Poly(thiophene)-graft-poly(acrylate urethane), *Soft Matter* **14**, 6875-6882 (2018) (from BILBY, PLATYPUS) [DOI](#)
9. Brice, CA; Tayon, WA; Newman, JA; Kral, MV; Bishop, C and Sokolova, A, Effect of compositional changes on microstructure in additively manufactured aluminum alloy 2139, *Mater. Charact.* **143**, 50-58 (2018) (from BILBY) [DOI](#)
10. Jang, JD; Bang, J; Han, YS; Sokolova, A and Kim, TH, Phase behaviors of a mixture of two kinds of Pluronic triblock copolymers in aqueous solution, *Phys. B* **551**, 184-190 (2018) (from BILBY) [DOI](#)
11. Jiang, B; Guo, Y; Kim, J; Whitten, AE; Wood, K; Kani, K; Rowan, AE; Henzie, J and Yamauchi, Y, Mesoporous Metallic Iridium Nanosheets, *J. Am. Chem. Soc.* **140**(39), 12434-12441 (2018) (from BILBY) [DOI](#)
12. Kelleppan, VT; Moore, JE; McCoy, TM; Sokolova, AV; de Campo, L; Wilkinson, BL and Tabor, RF, Self-Assembly of Long-Chain Betaine Surfactants: Effect of Tailgroup Structure on Wormlike Micelle Formation, *Langmuir* **34**(3), 970-977 (2018) (from BILBY) [DOI](#)
13. Kiani, A; Sakurovs, R; Grigore, M and Sokolova, A, Gas sorption capacity, gas sorption rates and nanoporosity in coals, *International Journal of Coal Geology* **200**, 77-86 (2018) (from BILBY) [DOI](#)
14. Lee, KJ and Yun, SI, Nanocomposite hydrogels based on agarose and diphenylalanine, *Polymer* **139**, 86-97 (2018) (from BILBY) [DOI](#)
15. Loy, CW; Whitten, AE; de Campo, L; Appadoo, D; Zainuddin, N; Matori, KA; Rehm, C; Sokolova, A; Wang, C; Xia, Q; Whittle, TA; and Schmid, S., Investigation of the siliceous hydrogel phase formation in glass-ionomer cement paste, *Phys. B* **551**, 287-290 (2018) (from BILBY) [DOI](#)
16. Marlow, JB; Pottage, MJ; McCoy, TM; De Campo, L; Sokolova, A; Bell, TDM and Tabor, RF, Structural and rheological changes of lamellar liquid crystals as a result of compositional changes and added silica nanoparticles, *Phys. Chem. Chem. Phys.* **20**(24), 16592-16603 (2018) (from BILBY) [DOI](#)
17. McCoy, TM; De Campo, L; Sokolova, AV; Grillo, I; Izgorodina, EI and Tabor, RF, Bulk properties of aqueous graphene oxide and reduced graphene oxide with surfactants and polymers: Adsorption and stability, *Phys. Chem. Chem. Phys.* **20**(24), 16801-16816 (2018) (from BILBY, KOOKABURRA) [DOI](#)
18. Moore, JE; McCoy, TM; de Campo, L; Sokolova, AV; Garvey, CJ; Pearson, G; Wilkinson, BL and Tabor, RF, Wormlike micelle formation of novel alkyl-tri(ethylene glycol)-glucoside carbohydrate surfactants: Structure-function relationships and rheology, *J. Colloid Interface Sci.* **529**, 464-475 (2018) (from BILBY, KOOKABURRA, QUOKKA) [DOI](#)
19. Sakurovs, R; Koval, L; Grigore, M; Sokolova, A; Ruppert, LF and Melnichenko, YB, Nanometre-sized pores in coal: Variations between coal basins and coal origin, *International Journal of Coal Geology* **186**, 126-134 (2018) (from BILBY) [DOI](#)
20. Sakurovs, R; Koval, L; Grigore, M; Sokolova, A; de Campo, L and Rehm, C, Nanostructure of coals, *International Journal of Coal Geology* **188**, 112-120 (2018) (from BILBY, KOOKABURRA) [DOI](#)
21. Subianto, S; Balu, R; De Campo, L; Sokolova, A; Dutta, NK and Choudhury, NR, Sulfonated Thiophene Derivative Stabilized Aqueous Poly(3-hexylthiophene):Phenyl-C61-butyric Acid Methyl Ester Nanoparticle Dispersion for Organic Solar Cell Applications, *ACS Appl. Mater. Interfaces* **10**(50), 44116-44125 (2018) (from BILBY, KOOKABURRA) [DOI](#)
22. Baek, P; Aydemir, N; An, Y; Chan, EWC; Sokolova, A; Nelson, A; Mata, JP; McGillivray, D; Barker, D and Travas-Sejdic, J, Molecularly Engineered Intrinsically Healable and Stretchable Conducting Polymers, *Chem. Mater.* **20**(29), 8850-8858 (2017) (from BILBY) [DOI](#)
23. Iqbal, M; Li, C; Wood, K; Jiang, B; Takei, T; Dag, Ö; Baba, D; Nugraha, AS; Asahi, T; Whitten, AE; Hossain, MSA; Malgras, V and Yamauchi, Y, Continuous Mesoporous Pd Films by Electrochemical Deposition in Nonionic Micellar Solution, *Chem. Mater.* **29**(15), 6405-6413 (2017) (from BILBY) [DOI](#)

Bilby, Quokka, Kookaburra references

- “Performance and characteristics of the BILBY time-of-flight small-angle neutron scattering instrument”

Sokolova A. et al, J. Appl. Crystallography , 52, p.1-12 (2019)

- “QUOKKA, the pinhole small-angle neutron scattering instrument at the OPAL Research Reactor, Australia: design, performance, operation and scientific highlights “

Wood, K et al, J. Appl. Crystallography , 51(2), p.294-314 (2018)

- “Design and performance of the variable-wavelength Bonse–Hart ultra-small-angle neutron scattering diffractometer KOOKABURRA at ANSTO”

Rehm C. et al, J. Appl. Crystallography, 51(1), p.1-8 (2018)

User access

<https://www.ansto.gov.au/research/facilities/australian-centre-for-neutron-scattering>

Neutrons proposals call: twice a year, 15 March & 15 September

<https://www.ansto.gov.au/research/facilities/national-deuteration-facility>